UNIVERSITÀ DEGLI STUDI DI TRIESTE

XXXIV CICLO DEL DOTTORATO DI RICERCA IN

Scienze della terra e meccanica dei fluidi

Titolo della Tesi

Speleoseismology in the Dinaric Karst of Slovenia

Settore scientifico-disciplinare:

GEO/10 GEOFISICA DELLA TERRA SOLIDA

DOTTORANDO: **Donna M. Bou-Rabee**

COORDINATORE: **Prof. Stefano Maset**

SUPERVISORE DI TESI: **Prof. Abdelkrim Aoudia**

ANNO ACCADEMICO 2020/2021

Speleoseismology in the Dinaric Karst of Slovenia

Bou-Rabee Donna
University of Trieste

A Thesis submitted for the degree of
Doctor of Philosophy

November 2021

Abstract

Cave sediments may be used not only as archives for past climate changes but also as an important and until recently overlooked archive for seismic events. This has been done in many karstic areas around the world, but not in the Dinaric Karst area of Slovenia making this study a pioneer work. The Dinaric Karst covers the area between the Ljubljana Marsh (Slovenia) to the east and the Bay of Trieste (Italy) to the west and Rijeka (Croatia) to the south. There are around 6,000 known and explored caves and other karstic phenomena in this area that covers approximately 6,400 km^2 or 27% of the territory of Slovenia. In the present study, speleothems from several caves in the Slovenian part of the Dinaric Karst area are sampled (more than 90 samples were taken and analyzed) and so far 34 were dated using the radiometric U/Th method. The sampling excluded deformed speleothems other than seismically deformed ones therefore validating the samples as records of paleoearthquakes. Two temporal clusters (around 3kyr BP and 10kyr BP) could be identified from our results. Therefore, the the Dinaric Karst in Slovenia was not only affected by the 1511 magnitude 6.9 historical earthquake sequence but most likely also by two newly inferred large paleo earthquakes.

Keywords: Dinaric Karst, speleothems, U/th dating, paleoearthquakes, speleoseismology.

Table of Contents

1 Introduction

Cave sediments may be used not only as an archive for past climate changes but also as an important and until recently overlooked archive for seismic events. Reports of probable earthquake effects in caves date back to the early 20th century. Documented studies of seismic event effects in caves started to emerge in scientific journals in the 1960s (McCalpin, 2009). While this has been done in many places around the world, the method is relatively new to the seismically active north-eastern Mediterranean, especially to the Dinaric Karst territory, north-western Dinarides. Dinaric Karst covers the area between the Ljubljana Marsh (Slovenia) to the east and the Bay of Trieste (Italy) to the west and Rijeka (Croatia) to the south (Kranjc, 1997). There are around 6,000 known and explored caves and other karstic phenomena in this area that covers approximately 6,400 km2 or 27% of the territory of Slovenia.

In the present study, speleothems, cave sediments, from several caves in the Dinaric Karst area in south-western Slovenia are sampled and dated using the radiometric U/Th method. The data are then correlated with known seismic events and their feasibility as paleo seismic archives is verified.

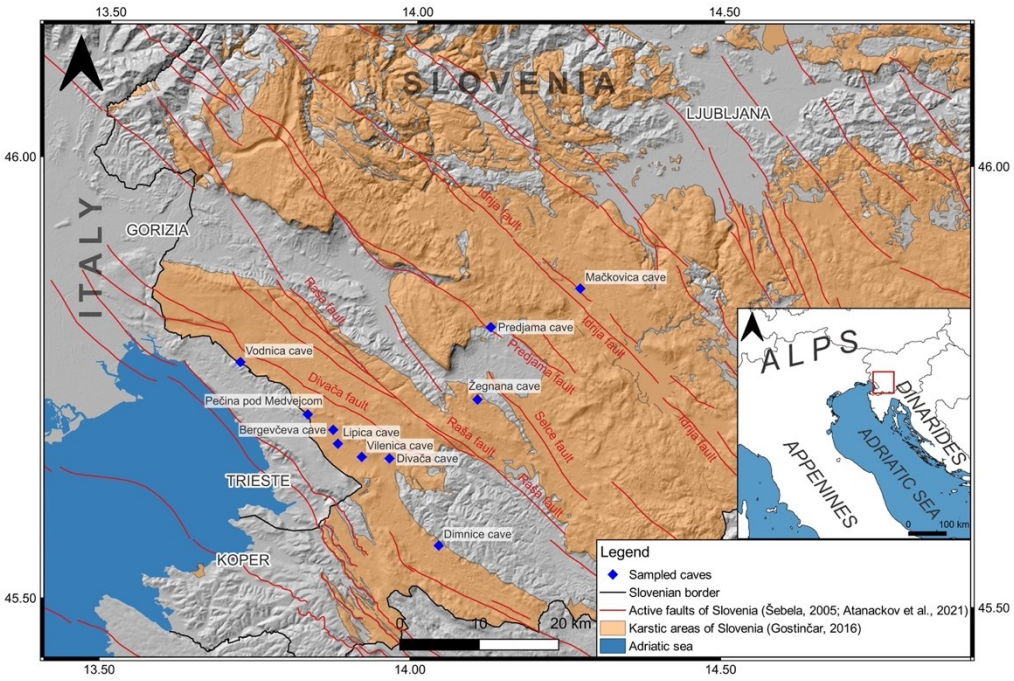

Fig. 1: Map of the study area, with sampled caves locations, active fault traces and karstic areas

The study area (Fig. 1) belongs to the North-western Dinarides and is crossed by the Dinaric fault system, a system with several dextral strike-slip active faults in a NW-SE trending direction such as the Raša fault and the Idrija fault. There are known historic seismic events in this area as well as instrumental records from this area. One example is the historical event of the 1511 Idrija earthquake with a magnitude of ~ M 6.9 on the Idrija fault and the another is the more recent seismic event of 1998 (Md=5.6) on Ravne fault (Vičič et al., 2019). Besides the two mentioned earthquakes, there are other known historic earthquakes in the wider area. These include the 1998 Ms 5.7 Bovec and 2004 Ms 5.4 and the 1956 ML 5.1 and Mw 4.5 earthquakes (cited after Vicic 2017). The study area also has effects of historical seismic events. According to Šebela (2010), the 1st January, 1926 earthquake (Mw=5.6) led to the collapse of a stalagmite column of 1 m in diameter. Such a large damage is very rare

in karst caves and possibly it only took place because the epicenter was in the very vicinity. In addition, there are modern paleo seismic studies where seismic records from surface-near trenching have been investigated (Grützner et al. 2021).

2 Methods

All the caves are situated in Mesozoic carbonate rocks, spanning from Lower to Upper Cretaceous. The main selection of the ten sampled cave sites was based on geographical location, their vicinity to the major seismically active NW-SE trending fault zones and their spatial distribution crosswise (SW-NE) the fault zones. Thus permitting the use of data for regional paleo seismic event interpretation in the study area. Before a seismic origin of the deformed speleothem can be inferred, all other possible causes of the disturbance must be ruled out. Therefore the sampling sites of speleothems in the caves were selected in a manner that they excluded any signs of biogenic or anthropogenic impacts, effects of sediment subsidence or landslides, impacts of ice flows, effects of the outside climate (freezing-thawing cycles) and impacts of running water (Shanov and Kostov, 2015).

The selected speleothems show clear signs of seismic disruption such as breakage or even just a distinct change in growth direction. According to suggestions from literature, the sampled speleothems should be cylindrical stalagmites. Most of the sampled speleothems were sampled in caves' dry collapse chambers. They were situated on older structures, fallen bedrock blocks, pillars and stalactites. The sampled speleothems that inferred the same event had to exhibit uniform growth characteristics, size and shape, and had to belong to a group that had a sufficient number of deformed

speleothems, which allow statistical analysis (Shanov and Kostov, 2015). Samples from horizontal surfaces were preferred to minimize influence of gravity. Such an influence could lead to secondary redeposition and has a higher likelihood on non-horizontal surfaces.

Samples from ten different caves were taken by using an electrical drill with a diamond core drill bit from the contact between pre-event sediment and post-event sediment. The diamond core drill bit was used to ensure minimal destruction of the speleothems. The situation before and after sampling was documented photographically. The locations of all sampled speleothems were documented and logged on the cave map and cave profile. As per nature conservational legislature of Republic of Slovenia a sampling permit was acquired for each cave and a report of sampled speleothem sites was submitted to the Institute of the Republic of Slovenia for Nature Conservation.

The speleothem samples were prepared and dated at the laboratory at the University of Oxford. Prior to the preparation, a little chip of sample of around 100 mg was cut using a saw blade mounted on a “Dremel” tool in the preparation laboratory. The measurements were carried out with a Thermofinnigan element 2 ICP-MS instrument.

Speleothems and Sampling Technique

Deformed, broken and collapsed speleothems in caves can form as a result of multiple reasons. In our study, the sampled speleothems were chosen accordingly to directions and procedures published by Šebela (2004) and Kostov & Shanov (2015). We excluded deformed speleothems, which could have formed from reasons other than seismic activity. Examples of processes behind deformed speleothems are:

- Biogenic or anthropogenic activity; traces of negative human impact is normally represented as broken stalagmites and stalactites in easily accessible, entry parts of the caves. Anthropogenic activity can be easily recognised. Occasionally there is a negative destructive biogenic impact on speleothems as a result of activity of Pleistocene large mammals. This can be distinguished by the presence of fossil bones.
- Effects of subsidence and gravitational processes; if the speleothems are forming on fluvial or colluvial sediments they can be inclined, collapsed or broken.
- Impacts of ice movement; this applies only for karst areas near the snow lines during ice age conditions of the Pleistocene and to contemporary ice caves.
- Effects of the outside climate; freezing-thawing cycles at the entry parts of the caves can result in broken and collapsed speleothems and rock falls.
- Impacts of running water; hydrological active parts of caves should be avoided. Speleothems could be broken due to torrent flows.

At first, a suitable speleothem was identified in the cave, avoiding previously described scenarios. According to Akgöz & Eren (2013), cylindrical stalagmites with uniform growth in sufficient numbers should be the preferred specimens for paleo seismological studies. They state, that these samples usually work best because they have not been affected by changing hydrological and chemical conditions. A change in grow rate could suggest a change in the precipitation pattern and would in this way prohibit the use of such a speleothem for analysis of earthquake influence. Changing grow rate of speleothems could also be influenced by changes in water chemistry such as pH or the amount of dissolved carbonates or in physical parameters such as changes in water temperature.

Only speleothems which were cemented to the cave floor were sampled, as lose speleothems could have been changed post seismically for example by human impact or gravitational processes (Delaby (2001)). In accordance with Delaby (2001), samples from horizontal surfaces were preferred to minimize influence by gravity. The selected speleothems should be calcified to an older generation of secondary formations, so there is relative age evidence of events that caused the deformation.

As per nature conservational legislature of Republic of Slovenia all the caves in Slovenia are protected by the law and registered under “The Register of valuable natural features”. Therefore, a sampling permit was acquired from the Slovenian Environment Agency for all of the sampled caves. After each cave sampling a detailed report of each specimen micro-locations including photographs of pre- and post-sampling situation was submitted to the Institute of the Republic of Slovenia for Nature Conservation.

Samples in this study were taken at the contact between pre-event sediment and post-event sediment (Fig.):

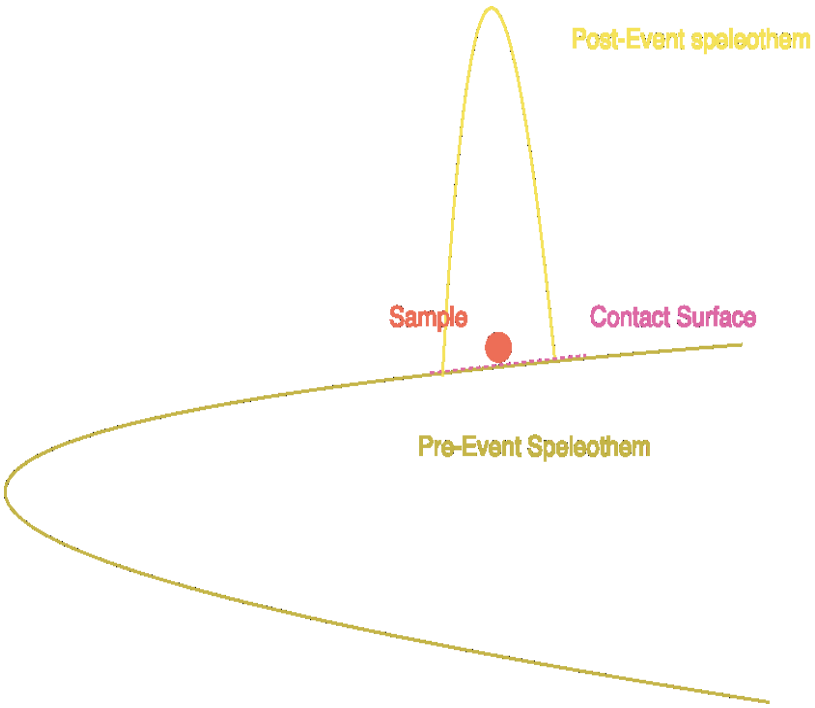

Fig. 2: Sketch of the sample location (drawing by the author)

Fig. 3: Sampling using a battery drill, ensuring minimum destruction of the speleothem

At first, samples were taken with a hammer and a chisel. Every sampling of the speleothem with aforementioned destructive technique needed a lot of consideration regarding the positioning of the sample and minimizing the impact on the natural

setting. in it. Later on samples were taken using a 20 mm diamond covered core bit riven by a cordless, battery 18V- drill (Fig.). This is a method described for example by Kagan (2012) and Spötl & Mattey 2012. While a 5 mm diameter drill-bit would be sufficient for dating (Speleothem Science working group at the Schools of Earth Sciences and Geography at the University of Melbourne, Australia), the larger sample size allows for both dating and for further investigations of the structure of the core. Using the drill instead of a hammer minimizes the destruction of the fragile cave environment and is therefore preferred. After the cores were drilled, they were broken close to its base and then removed from the borehole. The drill hole was meticulously rinsed with water in order to cover any signs of human impact. and the cores were brought to the surface.

The micro-locations of all taken samples were documented on the cave maps, mostly ground plans and cave cross-sections if they were available. Additionally, the sampled micro-location situations before and after sampling were documented photographically.

To take into account the disadvantages of taking drill cores such as only showing a small part of the speleothem and thus making interpretation of spatial changes difficult (Becker et al. 2006), the micro-setting of each sampling site in the cave was documented thoroughly. In that way, the small samples could give a good representation of spatial changes.

The subsamples were taken using a rotary drilling tool known as “Dremel” drill with diamond covered cutting drill-bit.

2.1 Radiometric Dating Techniques of Speleothems

2.1.1 General Information on the Dating Method

Dating can be carried out by different methods. As carbonates contain carbon, geologically young sediments can be dated using the radiocarbon method (e. g. used by Becker et al. 2005). For older sediments, U-Th-Pb dating can be used (e. g. Kagan 2012). If even older sediments need to be dated, the U-Pb series can be used, enabling the dating of sediments as old as 10 Myr (Woodhead et al. 2016). Besides using these radiometric dating methods, it is also possible to use paleomagnetic reversals as time markers and this technique has for example been used by Sasowski et al. (2003).

Besides dating the carbon in the carbonate, also organic micro remains within sediments can be dated. The results need to be corrected for "dead carbon" which is carbon from the surrounding limestone. According to Becker et al. (2012), samples containing dispersed organic material need to be wet sieved and then treated by an acid-alkali-acid (AAA) pre-treatment. This treatment consists of 4% HCl for 30 minutes, then 3 steps of 4 % NaOH for a period of one hour and finally 4% HCl for another hour. According to Becker et al. (2012) material should be centrifuged between each step.

Samples from the carbonate are dissolved in acid (HCl) and the resulting CO_2 is collected and converted to graphite.

Finally the $^{14}C/^{12}C$ ratio is measured, due to small sample sizes and relatively old samples, this measurements needs to be carried out by accelerator mass spectrometry (AMS). Laboratories for AMS radiocarbon dating exist at several institutes, for

example at Lund University in Sweden, in Heidelberg, Cologne, Kiel in Germany, and Zürich/Hönggerberg in Switzerland.

For U-Th-Dating, the amount of material needed depends on the uranium concentration. The sample is then dissolved in 7N HNO_3 and thereafter spiked with a ^{236}U-^{229}Th spike (Kagan 2012). The U and Th of the carbonate fraction of the speleothems are chemically separated using chromatography and then the isotopes ^{238}U, ^{234}U, ^{230}Th and ^{232}Th are measured by a Multi-Collector Inductively Coupled Plasma Mass Spectrometer (MC-ICP-MS). To test the instrument performance, a standard reference material for U isotope ratio measurements needs to be used. The isotopic mass discrimination of the instrument also needs to be corrected for.

The U-Th dating method assumes that all ^{230}Th present in the calcite is formed within the speleothem by radioactive decay of uranium which co-precipitated with the calcite. This is not the case in speleothems where Thorium may also have been added by the integration of detrital material such as clay. Therefore, the measured data need to be corrected for detritus (Kagan et al. 2017).

After the correction, the ^{230}Th /^{234}U age is calculated (Becker et al. 2012). The U-Th-measurements in their study were carried out at Heidelberg University while Kagan et al. (2017) used the laboratory of the Geological Survey of Israel. Another laboratory where U-Th-dating may be carried out is the laboratory of Prof Gideon Henderson, research group on Isotopes and Climate, Department of Earth Sciences at the University of Oxford.

In the paper by Sasowski et al. (2002), samples are taken for paleomagnetic analyses in plastic cubes and their spatial orientation is noted. In the laboratory, the samples are magnetically cleaned in a stepwise alternating field (AF) demagnetizer and are then measured in a large-bore, 3-axis 2-G superconducting rock magnetometer (SRM). By inspecting the plots and using principal component analysis, the characteristic remnant magnetic vector is determined. In addition to this vector, the samples are also analyzed for magnetic susceptibility and isothermal remnant magnetization. Paleomagnetic laboratories exist at institutes such as the University of Pittsburgh, the University of Liverpool, and Lund University.

Delaby (2001) suggests that a broken stalagmite on which a new stalagmite developed is a good source for age data. If both the oldest part of the new stalagmite and the youngest part of the fallen stalagmite are dated, it is possible to construct minimum and maximum ages for the rupture and thus for the event (e. g. the earthquake) which led to the creation of the rupture. To exclude dating errors, also the dating should be performed on a sufficiently large number of speleothems and the age data should then be averaged.

2.1.2 Laboratory Procedures

2.1.2.1 Beaker preparation

Teflon beakers are taken to the clean laboratory and filled partially with 8M reagent grade nitric acid. The beakers are covered and are cleaned with the acid overnight at 130°C before they are rinsed three times with ultrapure water (18MΩ resistivity).

Afterwards the beakers are filled completely with nitric acid, a lid is put on them and then the beakers are cleaned for another night, also this time at 130°C.

2.1.2.2 Resin preparation

For the analyses in this study, 100-200 mesh resin is used. A clean bottle is filled to a level of 10-20% with the resin and afterwards the bottle is filled to the top with ultra pure water and shaked well. The resin is allowed to settle by gravity and as much water as possible is decanted from the bottle. The process is repeated 2-3 times or until the water is clear and no more foam is forming.

After washing the resin with water, new water is added to 3/4 of the bottle and 20-50ml HCl is added before the bottle is filled with water to the top and shaked. After allowing the sediment to settle, the acid-water mixture is removed by decanting.

After the cleaning with diluted HCl, another 3-4 cleaning steps using water (see above for detailed procedure) are executed.

Finally water is added to the bottle and a small amount of HCl is added. Then the columns may be stored until using them.

2.1.2.3 Column preparation

The columns used for U-Th and U-isotope measurements in carbonates are 2 ml Biorad columns. They are stored in ultra clean water. To prepare them they are first immersed for 1-2 hours in 8N HNO_3 (50% by volume) and then cleaned with water. Afterwards they are immersed in 6N HCl (50% by volume) for another 3-4 hours. Afterwards they are left in a PP wide neck bottle and are covered with 2N HCl at room temperature overnight.

After cleaning the lab and the hood properly using 18MΩ water the columns are taken from their storage vessel and are rinsed 3 times using 18MΩ water. Then the columns are put into the column rack. A waste beaker is placed beneath each column and 2ml of resin is added to the columns using a 5ml pipette.

The resin is then washed with 7.5 M HNO_3 followed by 2% HNO_3 and 7.5 M HNO3 and another round of 2% HNO3. Afterwards the resin is washed with 6M HCl followed by ultrapure water. The columns are then conditioned with 2x5 ml of 7.5M HNO_3.

2.1.2.4 Sample preparation for dating

For preparing the samples, a little chip of sample (around 100mg) is cut using a saw blade mounted on a “Dremel” tool in the preparation laboratory. The chip is moved to the clean laboratory and put into a bottle and rinsed with 18MΩ ultrapure water in an ultrasound bath. Afterwards the water is removed and new ultrapure water with around 2 % 8M nitric acid is added. The beaker is put back into an ultrasound bath for another minute. Afterwards, the diluted acid is removed and replaced by ultrapure water for another 1 minute ultrasound treatment.

To take into account for the loss of material in column chemistry, a carbonate spike with known 236U/229Th ratio of .554 g is split into 11 parts of 50mg and added to each sample. The spike is added using to the beakers using a pipette 20-200µl with a tip size 50-1000µl).

Afterwards 400µl of 16 molar nitric acid are added to each beaker to convert the sample into nitrate form, and the beaker is then covered with a lid. After standing on

the hot plate at 130°C over night to equilibrate, the lid is removed, and the nitric acid is evaporated.

The samples are loaded into the column directly from the sample beaker. The column is then washed with 2x5 ml of 7.5M HNO3. The column is then converted with 4x 0.25 ml and 1x 0.5ml of 6M HCl. As the spike is radioactive, the waste from these steps needs to be treated as radioactive waste.

The Thorium cut is eluted with 2x1 ml and 2x2 ml of 6M HCl. The Uranium cut is eluted with 2x1 ml and 1x4 ml of H2O.

Each cut is dried down in an oven without boiling it. 0.2 ml of concentrated HNO3 is added and the sample is dried down. The dried sample is dissolved in 42µl of 7.5N HNO3 and stored for mass spectroscopy.

0.2 ml of 2% HNO3 is added to the sample and the sample is put on a hot plate at 100°C over night before the uranium measurement. When the samples are dry, another 1 ml of HNO3 is added to the beaker.

The Th sample beakers are covered and put on 80-90°C hot plate overnight.

In preparation for mass spectroscopy, the samples are then transferred to Eppendorf tubes.

2.1.2.5 Sample preparation for uranium concentration measurement

For uranium concentration, a hole is drilled into the sample and around 500 µg of drilling powder is collected for analysis. Around 250 µg of the sample is then weighed and collected on a clean piece of foil.

2.1.2.6 Measurements

The measurements are carried out using a THERMOFINNIGAN ELEMENT 2 ICP-MS instrument at the laboratory of Philip Holdship at the University of Oxford.

The samples are loaded into an auto sampler and are pumped into a sample chamber as a fine mist.

Inside the MS, a plasma at 10,000 Kelvin is created. The plasma desolvates atomizes and ionizes the sample which is then formed into a beam of highly energized particles by use of electromagnetic. The ions are accelerated in a high vacuum environment and are then filtered according to their mass to charge ratio (m/z) and are then sequentially detected by a secondary electron multiplier.

2.1.2.7 Calculation of concentrations

The weight (in grams) of the sample is determined and the volume of the solution (5 ml -> 5 grams) is divided by the weight of the sample, and the result is the dilution factor.

The measured concentration of uranium is multiplied by the dilution factor to calculate the concentration of uranium in the rock sample.

3 Scientific Background

3.1 Prerequisites for the formation of karsts

Karst is a landscape type which is formed by the chemical dissolution of rocks. Mainly soluble carbonate rocks such as limestone, dolomite and gypsum are susceptible to this type of dissolution. However, karstic landscapes can form even in metamorphic rocks, such as quartzites.

A speleothem is an autochthonous “in situ” cave deposit or cave formation. According to Forti & Onac (2016), a speleothem can consist of any secondary mineral deposited within a cave, regardless of the composition or external shape or internal crystal structure. This is in contrast to early research where only calcium carbonate deposits were subsumed under this term. Later on, also gypsum deposits were included in the term of speleothems.

The most important characteristic of karst landscapes is subterraneous water drainage. A large part of the drainage may flow via subterraneous cavities and caves. Surface water flow may be limited by sinkholes, making rivers and lakes a rare occurrence in karst type terrain. Karst phenomena are quite common on a global scale with 44% of Slovenia, 30% of Europe and 20% of the world being covered by karst.

While also other processes for mineralization exist, chemical dissolution and precipitation are the dominant processes in karst landscape evolution. The process formula $CaCo_{3(s)} + H_2O + CO_{2(g)} \rightleftarrows Ca^{2+}_{(aq)} + 2HCO_3^-$ can be read in both ways.

If the formula is read from left to right it describes the dissolution of calcium carbonate by meteoric water (i. e. precipitation such as rain) which is acidified during its passage

through the soil. This chemical dissolution is the main process for the formation and other karst features.

While this dissolution is enough to create small dissolution forms in the limestone, another process is mixture-corrosion (Bögli, 1963), which is crucial for the formation of larger dissolution forms and larger caves. Bögli (1963) described that two liquids which are saturated with calcium carbonate and which are mixed will act in a way which dissolutes limestone. This process is caused by the fact that the amount of dissolved calcium carbonate does not increase linearly with the concentration of dissolved CO_2 in water. The mixture of two $CaCO_3$-saturated solutions is not saturated with $CaCO_3$ and has therefore an excess of CO_2 which in turn will dissolve more $CaCO_3$ until the solution is saturated.

If the above mentioned process formula is read from right to left instead, the precipitation of calcium carbonate by degassing of the liquid and the formation of speleothems is described. Precipitation of carbonate occurs if CO_2 leaves the solution, i. e. if the CO_2 partial pressure drops.

If the carbonate-saturated water leaves the bedrock at the ceiling of a cave, CO_2 level drops and a stalactite starts to form. If the water drop which still contains carbonate reaches the floor of the cavity, further CO_2 is expelled which in turn leads to further precipitation of calcium carbonate and this is how the formation of stalagmites is induced.

As these processes are gravity-driven, formation of speleothems usually occurs in regular, often symmetrically shaped layers which mark different seasons. To create

significant changes in growth axis either the dripping point or the deposition point need to be moved.

As speleothems mainly occur in karst caves (with the name karst derived from the Kras [Italian: carso] region in Slovenia, much of the early karst research was carried out in this area. Other early karst research has been carried out in areas such as south west Germany and central and southern France (Gilli 1999).

3.2 Paleoseismicity Archives in Cave Deposits

When it comes to using speleothems as archives for paleo seismic processes, research has been carried out in Slovenia, but also in other areas around the world, such as the U. S. (Panno et al. 2009), Israel (Kagan et al. 2005) , Italy(Postpischl et al. 1991, Kagan et al. 2017, Di Domenica & Pizzi, 2017, Alfonsi & Cinti, 2021), Switzerland (Becker et al., 2005, 2012), China (Xueqin & Fudong, 2017), the Kamaun Himalayas (India) (Rajendran et al., 2016), the lower Tatra mountains in Slovakia (Szczygiel et al., 2021), the Carpathians in the Czech republic(Babek et al. (2015), Monaco(Gilli, 1999) among others.

In the 2009 book “Paleoseismology” by McCalpin, a very short overview on paleo seismic research on cave sediments (or as the author names it “speleoseismology”) is given, from the beginnings of the discipline to more recent developments. The author also writes about the importance of ruling out all other possibilities before inferring an earthquake origin of any structure in the cave.

In 2015, Shanov and Kostov published another monograph on the issue with the goal of providing a comprehensive monograph.

It has been reported from areas of low strain and infrequent damaging earthquakes, that cave features and speleothems may fail spontaneously without a triggering event. This possibility has been reported by Lang et al. 2021.

Panno et al. (2009) could show that cave sediments from southwestern Illinois and southeastern Missouri can be used as archives for earthquakes from the New Madrid Seismic Zone (NMSZ). According to the authors, the timing of the initiation and regrowth of stalagmites in southwestern Illinois and southeastern Missouri caves is consistent with the historic and prehistoric record of seismic events in the U.S. mid continent region. They conclude that dating the initiation of original stalagmite growth and later post-seismic-event rejuvenation may be used as paleo seismic method and that these methods may be used for caves all over the world.

There are several studies published for paleo seismic events in Israel which are related to the Dead Sea transform. Two examples for well-studied caves are the Soreq and the Har-Tuv caves which lie very close. A good example of paleo seismic research in Israel is given by Kagan (2012) where they analyzed two different types of archives: lacustrine sediments from the paleo-Dead Sea and speleothems from the two caves mentioned above. While the lacustrine sediments only cover a time span of 70 kyr, the speleothems provide a 400 kyr earthquake history. They analyzed damaged cave deposits such as collapsed stalactites, fallen stalagmites, standing but severed stalagmites, collapsed bedrock ceilings, cracked speleothems and collapsed soil mounds. The author distinguishes between pre-event sedimentation and post-event deposits which can also be called regrowth. To date the event, both pre-event and post-event sediments are sampled as close as possible to the contact and both samples are then dated by measuring the U-Th-Pb ratios by applying the MC-ICP-MS (Multicollector-Inductively Coupled Plasma Mass Spectrometer) method. The

acquired dates are then checked for errors and grouped into 26 groups which Kagan (2012) interprets to represent single events or earthquakes.

For Switzerland, Becker et al. (2005, 2012) could reconstruct several events from geological evidence. They could see records of the 1356 Basel earthquake, the 1601 Unterwalden earthquake and the 1774 Altdorf Earthquake in the record and used these events for calibration of the data. In total, they could find evidence for 13 earthquakes of M 6 or greater in their records. In the Becker et al. studies (2005, 2012), samples were dated by the radiocarbon method.

A study from the foreland of the Western Carpathians was published by Bábek et al. (2015), where they could show indication of a tectonic origin of the breakage of speleothems. By dating soft sediments with optically stimulated luminescence (OSL) and ^{14}C-dating, they could assign the events to a late Pleistocene to early Holocene age (MIS 2 to 1).

A general overview of the use of speleothems for seismo tectonic and paleo seismic studies has been published by Forti (2001). The author suggests that the study of speleothems may be used to reconstruct the location and epicenter of past earthquakes, their relative and absolute dating and their magnitude and proposes these studies to be used to improve seismic hazard evaluation.

While speleothem damage may be caused by seismic events of a larger magnitude, even moderate earthquake activity might be recorded in speleothems due to changes in the hydrogeologic conditions. Besides damaged speleothems, research may also be carried out on still growing stalagmites, as the growing axis may be perturbed by several factors such as the migration of the dripping point along a fracture on the ceiling and by gravity sliding of the stalagmite.

As a certain magnitude of an earthquake and a certain measure of horizontal movements is needed to fracture a speleothem, the presence of fragile but non-fractured speleothems such as soda straw speleothems in a cave is a sign for the absence of strong seismic events in that area (Bokelmann & Gribovszki, 2015). With knowledge about the mechanical properties of speleothems and their structural stability it is also possible to reconstruct a maximum magnitude of seismic events which they could resist. This can be an indicator of the maximum magnitude of seismic events which could have happened in the area, and which are not directly recorded in the speleothem. Every event with a magnitude that exceeds the stability of the speleothem would have destroyed it. Forti & Postpischl (1984) modeled stalagmites as simple inverted pendulums, which they then subjected to pseudo static engineering analyses.

Lacave et al. (2000) investigated the mechanical properties of speleothems and measured the natural frequencies and the damping on several different speleothems. They could show that most of the speleothems do not show dynamic amplification phenomena of the seismic motion because their natural moving frequency is higher than the frequency range produced by seismic events. A fundamental frequency higher than the seismic frequencies means that the speleothem moves, with its basement, as a rigid structure. The exceptions from these findings were extremely thin soda straw speleothems. According to Lacave et al. (2000), most of the broken speleothems are an indicator of the peak ground acceleration.

In another study, Lacave et al. (2004), measured the stability of speleothems by carrying out static bending tests on stalactites and soda straws. In this way, they could

measure the mean tensile resistance of the structure. The key finding of this study was, that not all speleothems have similar tensile strength but there is a large variation between the measured samples. These variations make it very complicated to estimate the acceleration necessary to break an individual speleothem. To overcome this issue, the authors developed a statistical approach which allowed them to study the speleothems and to estimate the probability that at least one moderate earthquake occurred in their study area.

It is also possible to use deformation structures in soft cave sediments as an archive. While the use of speleothems and other cave minerals as paleo seismic archives is a well-established field of research, there is also criticism to this method (Becker et al., 2006). Many of the critics attribute the fracturing of speleothems to other factors such as cave ice and thus argue that speleothems should not be used as archives for paleoseismic events. As Forti and Postpischl wrote in 1984 “the geological, morphological and speleogenetic analyses can be useful in distinguishing the various types of collapses that may be present in caves, even if such analyses will never be able to give a definitive certainty as to their cause “.

The focus of the critics differs a bit with Gilli (1999) putting the emphasis on creeping of cave ice and displacement of soft sediment. The author states that soft sediments in a cave are inflated during freezing and that they move gravity driven downwards slopes if the gallery is not horizontal. If a speleothem formed on this sediment, it is pulled down-slope and is in this way deformed or in cases of more pronounced displacement the speleothem is broken by that motion.

Kempe (2004) mentions some more possible causes for speleothem damages. The first cause mentioned is inkasion (rock fall) if sediments from the ceiling of the cave fall on sediments at the floor. Mass wasting can occur when limestone is formed on top of clay stone which can then act as a failure plane. The weight of stalagmite and flow stones can cause the underlaying soft sediment to compact, in turn leading to tilting of the stalagmite. Erosion of the sediment beneath a stalagmite can also cause tilting and breakage of the stalagmite. In caves which have been inhabited by animals or which have been open to humans, also biogenic factors and even vandalism need to be taken into account. Besides these reasons, Kempe (2004) also mentions cave ice as a cause for the destruction of speleothems, and one focus of this study is on how to reconstruct the zero-degree-line from the damaged speleothems.

One way of discriminating between speleothem fractioning by seismic activity or by ice movement is analyzing the way the fragments have been moved. While fragments produced by an earthquake may only have been moved by gravity or by major floods, the fragments produced by moving ice have been moved coherently during the flow (Kempe et al. 2009, Forti & Onac 2016).

Another possible method would be the shape of the breakage, with failure planes parallel to the stalagmite base being typical for fragmenting by a seismic event and seismic stress.

Mendecki and Szczygiel (2019) postulated that there is a correlation between the earthquake minimum magnitude required to damage a cave and the distance from the source of the earthquake. They estimated natural frequencies from P- and S-wave

moduli and describe the influences of caves depth on Peak Ground Acceleration (PGA) and give an introduction to the tunnel wave phenomenon in caves.

Gribovszki et al. (2018) simulated the oscillation of a given stalagmite by setting up four simplified models of the stalagmite. They measured the geometries of intact stalagmites in situ and the dimension of the fragments of broken speleothems in the geotechnical laboratory. They then calculated the eigenfrequencies of the stalagmites (the frequencies at which the stalagmite is prone to vibrate) and could in comparison to the measured stalagmites show that there is a splitting. This splitting could be reproduced in the calculation when the asymmetric shape of the speleothems was taken into account. They tested if intact stalagmites in caves can give important constraints on seismic hazard since they have survived all earthquakes over their (rather long) life span and argue that this can only be stated if the pattern of earthquake oscillation is fully understood.

3.3 Speleoseismicity and archives in Slovenia and the NW Dinarides

The very first observer that focused on the problematic of broken stalactites in Postojna cave was Hohenwart (1830), who wrote about them in his touristic cave guide.

The first scientific research of speleoseismicity in Slovenia was carried out in the 1960's in Postojna cave by Rado Gospodarič (1964, 1968). In his research on the morphology and cave deposits of the Postojna cave the author concludes that broken stalactites formed because of rockfalls, seismic activity or erosion of siliciclastic allochthonous cave sediments. Gospodarič (1964) found a fault in siliciclastic cave deposits in an artificial tunnel in Postojna cave with kinematic indicators, sinistral

strike-slip fault motion. Years later Sasowsky et. al. (2003) constricted the age of tectonic movements of the faults crosscutting sediments with paleomagnetism, to be younger than 780 ka.

Additionally, Sasowski et al. (2003) studied the directions of fallen stalactites in the Magical garden (Slovenian: Čarobni Vrt) in the Postojna cave and came to the conclusion that the stalactites in this cave do not show any preferable directions which could have formed due to seismic activity.

In 2008, Sebela notes, that most broken and non-ideal stalagmites are formed due to deformation of the unstable ground, which may be both caused by tectonic movements, seismic events but also by cryoturbation and cave ice. However, as reported by Sebela (2010), there are speleothem damages in the Postojna cave in Slovenia which can be clearly attributed to seismic events.

According to Sebela (2010), the 1st January, 1926 earthquake (M=5.6) led to the collapse of a stalagmite column of 1 m in diameter. The author admits that such a large damage is very rare in karst caves and that it only took place because the earthquake epicenter was in the very vicinity. While only strong and close earthquakes can be felt as ground shaking or waving inside the caves, weaker earthquakes induce brontides which can be heard inside the cave.

Zivcic et al. (2014) described the installation of a seismic station in the Postojna cave system. A first, temporary station was installed in May 2010 and was operational until 21 December 2010. In their paper, they also propose the installation of a permanent seismic station and give advice of where to install and how to operate it.

Grützner et. al (2021a, 2021b) investigated several surface paleoseismological trenches across the strike-slip Dinaric trending faults in Slovenia: Idrija fault, Raša fault and Selce fault. All the faults show signs of Holocene rupture deformations, younger than 15 ka.

4 Study Area

4.1 Geographical and Geological Setting

The study area is situated in the Dinaric Karst region in south-western Slovenia. The area is situated in NE Italy and W Slovenia at the transition between two different orogens, E-W trending Alps and the NW-SE trending Dinarides (Fig. 2). While caves are ubiquitous to most karstic parts of Slovenia, the highest density of caves is in the south-western region of Slovenia, called the Dinaric Karst (Fig. 3). Dinaric Karst covers the area between the Ljubljana Marsh (Slovenia) to the east and the Bay of Trieste (Italy) to the west and Rijeka (Croatia) to the south (Kranjc, 1997). It's comprised mostly of karstified Mesozoic carbonate strata. There are around 6,000 known and explored caves and other karstic phenomena such as karst polje, dolines etc. in this area that covers approximately 6,400 km^2 or 27% of the territory of Slovenia. The area of Dianaric Karst has a diverse relief, which strongly reflects the past and ongoing tectonic processes.

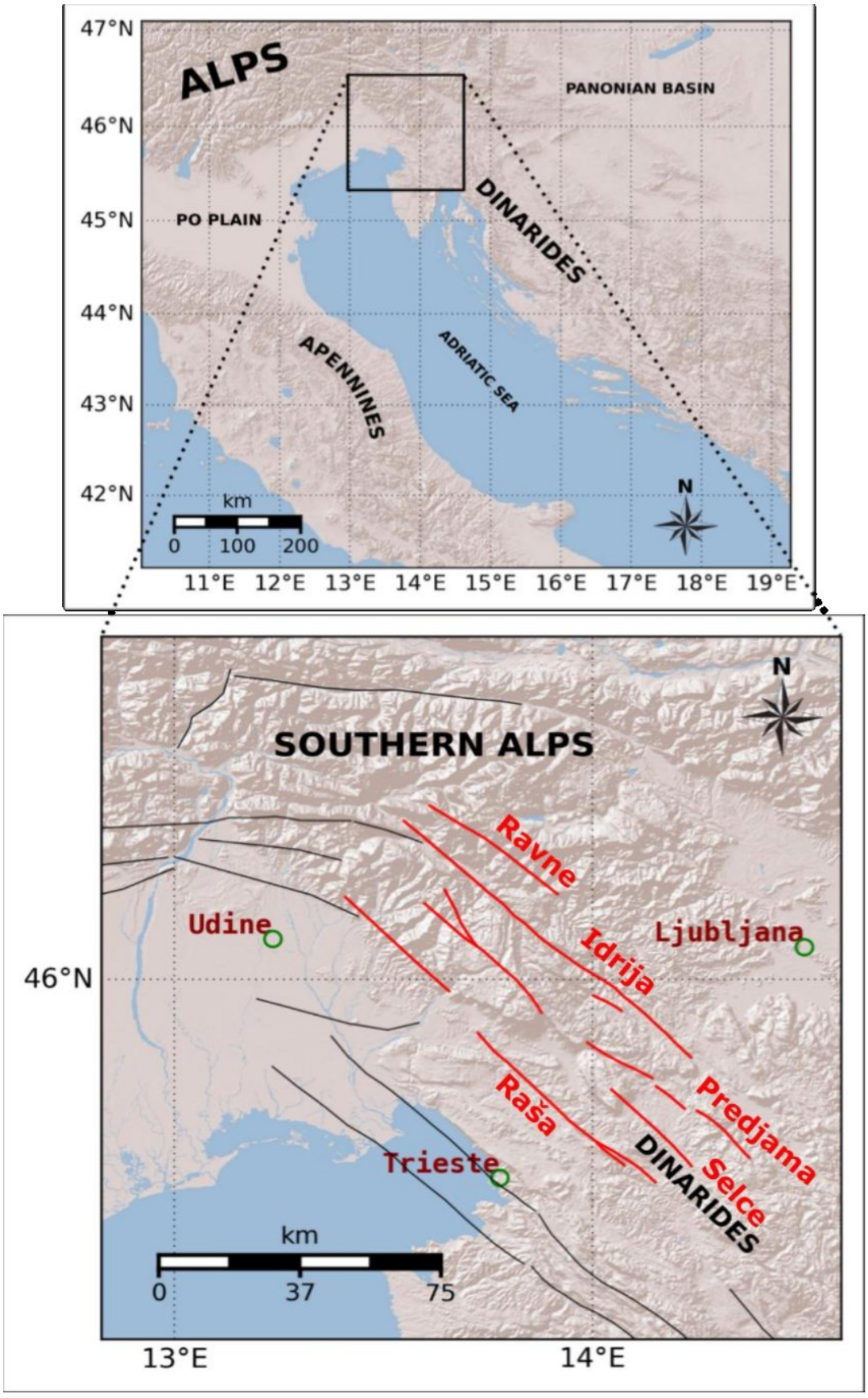

Fig. 2: Location of the studied area between two mountain chains, Alps and Di narides in the Western Slovenia. Black represents active faults from the DISS database (Roberto Basili et al., 2008) while red represents active faults of the Idrija fault system,from Vicic 2017.

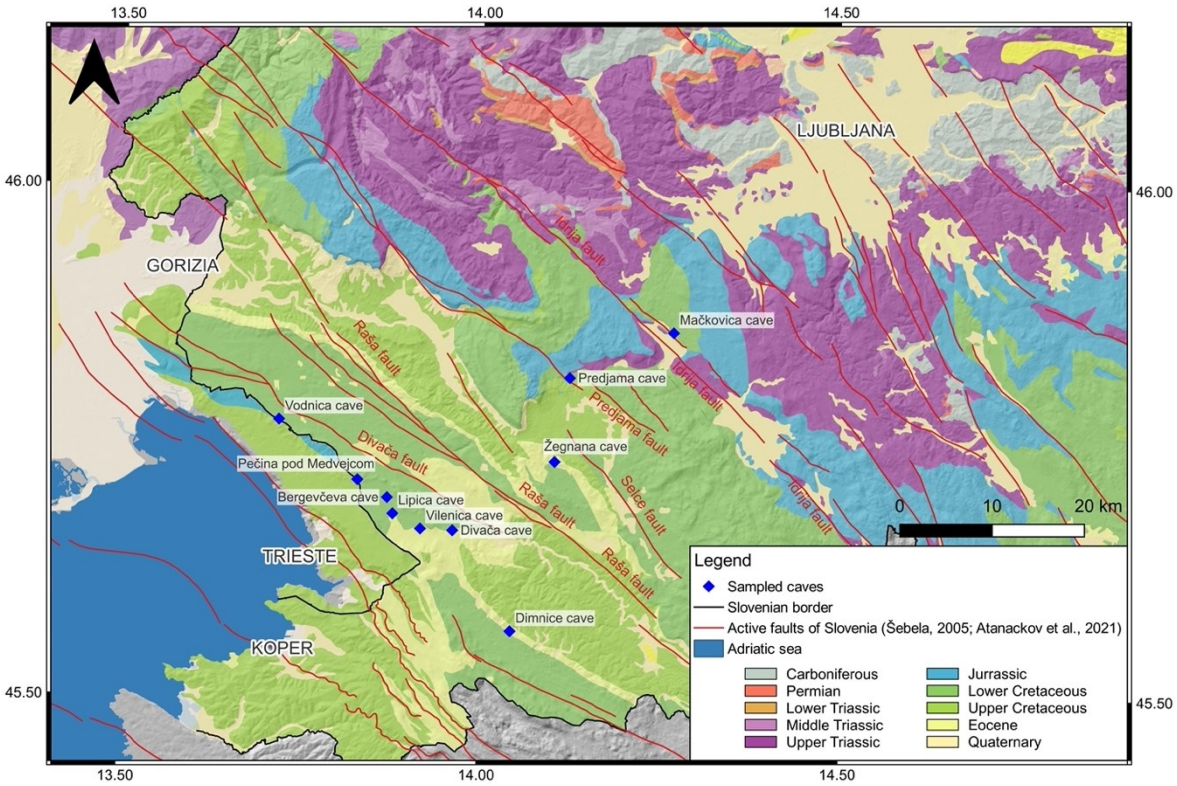

Fig. 3: Geological Map of Slovenia with sampled caves and active major faults marked. Geological Data from the Geological Survey of Slovenia, compiled by the author.

In morphological terms it forms the transition from the Po plain in northern Italy to the Julian alps which are the southernmost part of the Southern alps in the north and the Dinarides and the Dinaric Karst in the southern and south-eastern Part of the area.

From a tectonic point of view the study area is situated in the north-eastern corner of the convergent margin between the Adria and Europe and at the contact of two geotectonic units, namely the External Dinarides in the southern part and the southern Alps in the north of the studied area (Placer 1999, 2008; Placer et al. 2010) as seen on Fig. 4.

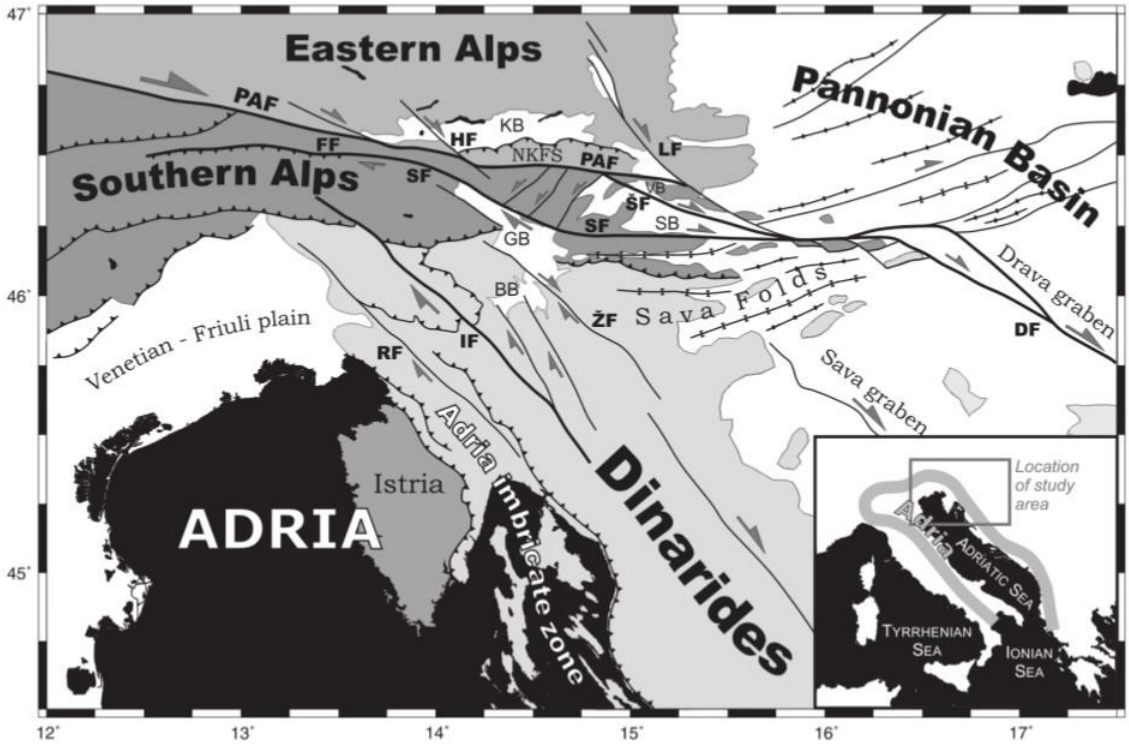

Fig. 4: Simplified tectonic map of the north-eastern corner of the Adria-Europe collision zone (Vrabec and Fodor 2006. The two- and three-letter-codes describe faults, relevant for this thesis are RF Raša fault and IF Idrija Fault Cited after Vicic 2017.

The study area is situated on the NE margin of the Adria microplate. Major tectonic units that characterize this region are E-W striking north dipping thrust sheet systems of the Southern Alps and from the NE part of the region, all along the central part of the area to its SE, NW-SE striking dextrally transgressing Dinaric fault system. The external front of the Southern Alps is situated north of the study area and contains a system of NE-SW striking, SE-verging thrusts through which strike slip and normal faults with the direction of NW-SE and NNE- SSW cut. These intersecting faults are a sign of older tectonic phases (Bressan et al. 2007). Towards E, the area is delimited by the Ljubljana Basin.

The oldest outcropping lithological units in the research area are Carboniferous and Permian mixed siliciclastic-carbonate rocks. The research area is primarily formed by

heavily karstified Mesozoic carbonate rocks and secondarily clastic rocks. The southern part consists of both Mesozoic carbonates and Tertiary, predominately siliciclastic rocks (flysch). Mesozoic carbonates paleo-geographically belong to the Adriatic Carbonate platform. Within the Dinaric fault system, mainly on the Idrija fault there are several pull-apart basins, which are mostly filled with younger Quaternary sediments (Buser, 2009).

The convergence between Africa and Eurasia is the main driver behind the regional geotectonic processes. When the Atlantic Ocean opened around 140Myr ago, the convergence in the study area started (Stampfli et al., 1998; Stampfli & Borel, 2002). The African promontory began to move independently from the African plate between 67-35 Myr ago, carving the Adriatic microplate between the European plate to the north the Iberian microplate to the west and the African plate to the south (Handy,et al. 2010). Around 40-35 Myr ago, the collision between the Adria microplate and the European plate started (Lippitsch, 2003; O'Brien, 2001; Stampfli et al., 1998; Stampfli & Borel, 2002), forming two orogens, the Dinarides at the north-eastern margin of the Adria microplate and the Alps at the northern margin of that microplate.

Data from precise GNSS technology gave us insights into recent geodynamic processes of the earth's surface. The measurements have shown that Africa is still actively converging with Europe at the rate of 4-6 mm/yr (Nocquet, 2012) (Fig. 5). In contrast, the Adriatic plate, started to move independently of Africa in a N-NW direction relatively to the stable Eurasia. This differential movement causes localized deformation along the boundaries of the plates which in turn triggers earthquake activity (Anderson & Jackson, 1987).

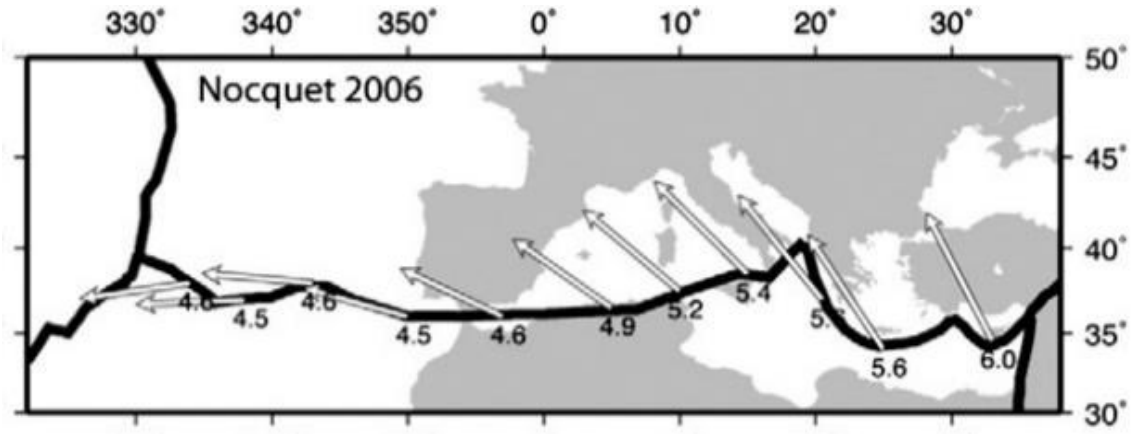

Fig. 5: Motion of Africa with respect to stable Eurasia from the geodetic datasets (Nocquet, 2012). Black lines represent plate boundaries, arrows represent motion vector of Nubia plate in respect to Eura sia plate in the last 3.16 Ma as predicted from the geological motion models

As shown by the GNSS vectors of the stations located in the Dinarides, in the Southern Alps and north of the Apennines indicate N movement (Nocquet 2012). A counterclockwise rotation of the Adriatic microplate is indicated by these measurements and a NE-SW extension along Apennines with a transition from N-S shortening in the Southern Alps to NE-SW shortening along the Dinarides are predicted. The deformation velocity is lower in the north and higher towards the south (Nocquet, 2012, Fig. 7).

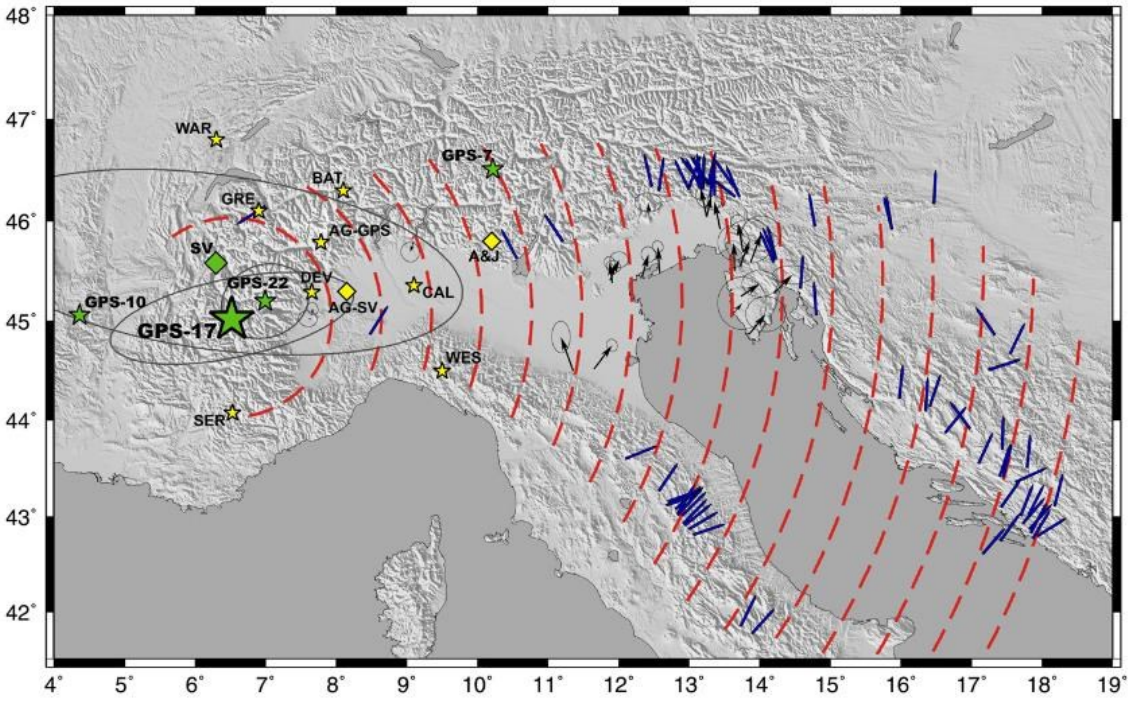

Fig. 6: Counter clockwise rotation of Adria with respect to stable Eurasia from GPS vectors and earthquake slip vectors (Weber et al., 2010) with approximate axis of rotation in the Western Alps.

When inverting the GPS vectors, the position of the rotation center of the Adriatic microplate relative to stable Eurasian plate to the Western Alps could be pinpointed. It could be shown that the angular velocity of the movement is 0.297 ± 0.116 / Myr (Fig. 6 from Weber et al., 2010). Most of the N-S shortening in the study area is absorbed in the Southern Alps (2-3 mm/yr) up to the Periadriatic line. On this line velocities decrease down to 0.5 mm/yr (Bechtold et al. 2009; Caporali et al. 2013; Grenerczy et al. 2000). When comparing between the single site RADO in N Slovenia and other sites along the Adriatic coast, it was found out, that there is up to 3 mm/yr of motion in a dextral direction along the NW-SE direction. In the Raša fault in W Slovenia around 1 mm/yr is accommodated (Caporali et al., 2013).

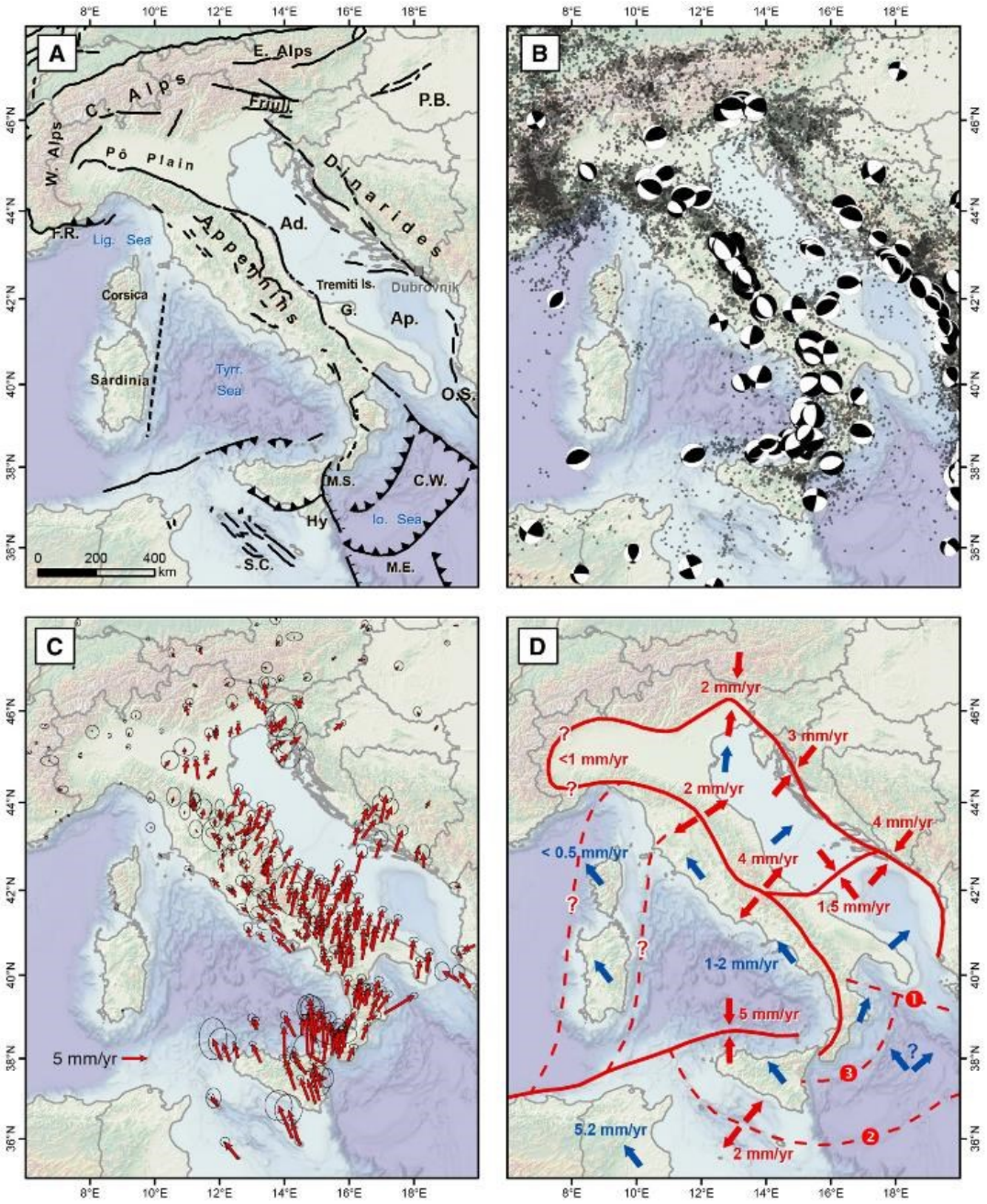

Fig. 7: a) tectonic map of the broader region, b) earthquak e distribution and their focal solutions, c) velocity field with fixed Eurasia, d) kinematic model of the Adria microplate (Nocquet, 2012).

4.2 Seismotectonic overview of NW Dinarides and current seismic activity

Slovenia is overall considered as a region with moderate seismicity, especially the western parts of Slovenia. Here we find the largest and most active faults in Slovenia present there, the regional dextral-strike slip faults, the so called Dinaric fault system (Atanackov et al. 2021). The fault zone is formed by several seismically active NW-SE trending faults which are the main focus of this study.

There are both known historic seismic events in this area as well as instrumental records of events (Fig. 8).

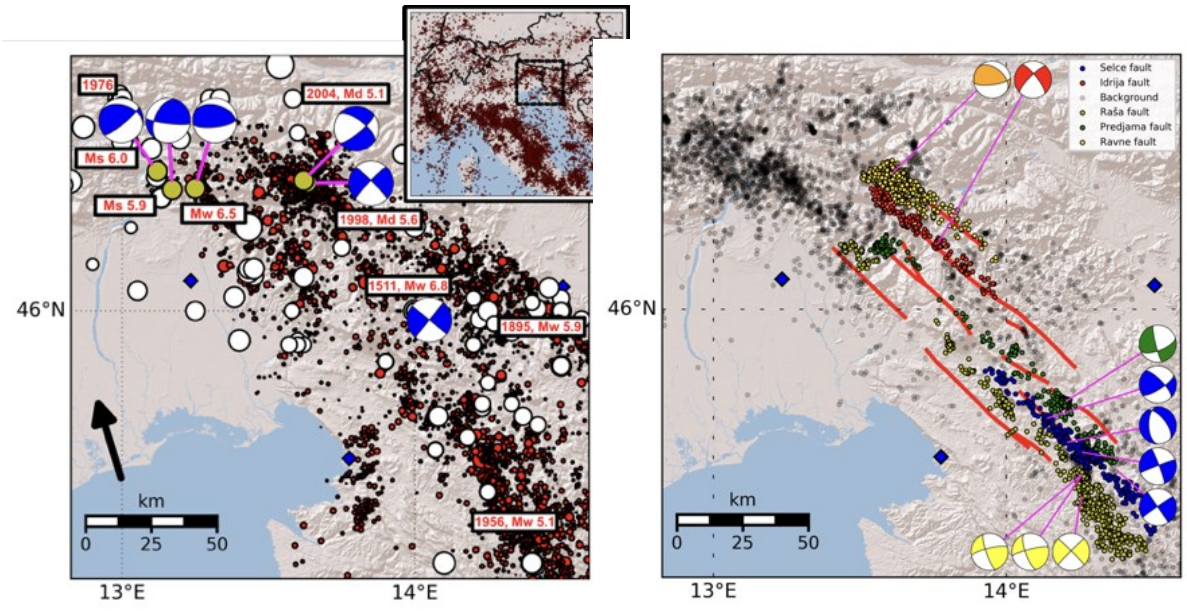

Fig. 8: Maps of the historic seismic events (left) and recently recorded seismic events (right), from Vicic et al. 2019

From digital elevation models it can be seen that several of the faults in the area are cropping out at the surface and that there is surface displacement in these places.

Recent activity of E-W trending N dipping thrust faults in the Southern Alps and NW-SE trending strike slip right-lateral faults in the Dinarides is suggested by the focal mechanisms of higher magnitude earthquakes which also caused destruction to speleothems (Aoudia et al. 2000; Bajc et al. 2001; Basili et al. 2013; Benedetti et al.

2000; Burrato et al. 2008; Fitzko et al. 2005; Galadini et al. 2005; Kastelic et al. 2004, 2008; Poljak et al. 2000; Ribarič 1982; Vrabec and Fodor 2006; Zupančič et al. 2001).

In the northernmost part of the Dinarides older thrust faults are present which are oriented in the NW-SE direction dipping towards the northeast.

There are also younger, active strike slip faults with the same direction and which are sub-vertical. The direction of the younger faults is inherited from the older structures (Kastelic et al., 2008; Placer, 2008a). These faults are named »Dinaric faults«, the name is derived from their orientation which is in the same direction as the older mainly compression related structures in the Dinarides. While they also mainly consist of NW-SE oriented NE dipping thrusts, they are not related to the Dinaric thrusting episode (Vrabec & Fodor, 2006). The whole fault system has a length of around 150 km and stretches between 46.3°N and 45.2°N along a N315 – S135 direction. Between the faults there is a separation zone consisting of 10 to 15 km of width with 10 to 18 km long segments (Moulin, 2014, Moulin et al., 2016).

While several of the strike-slip faults have a geomorphological expression and morphologic activity on the surface, only some of them show a direct connection to recent earthquake activity in the area. The other ones may be connected to older activity.

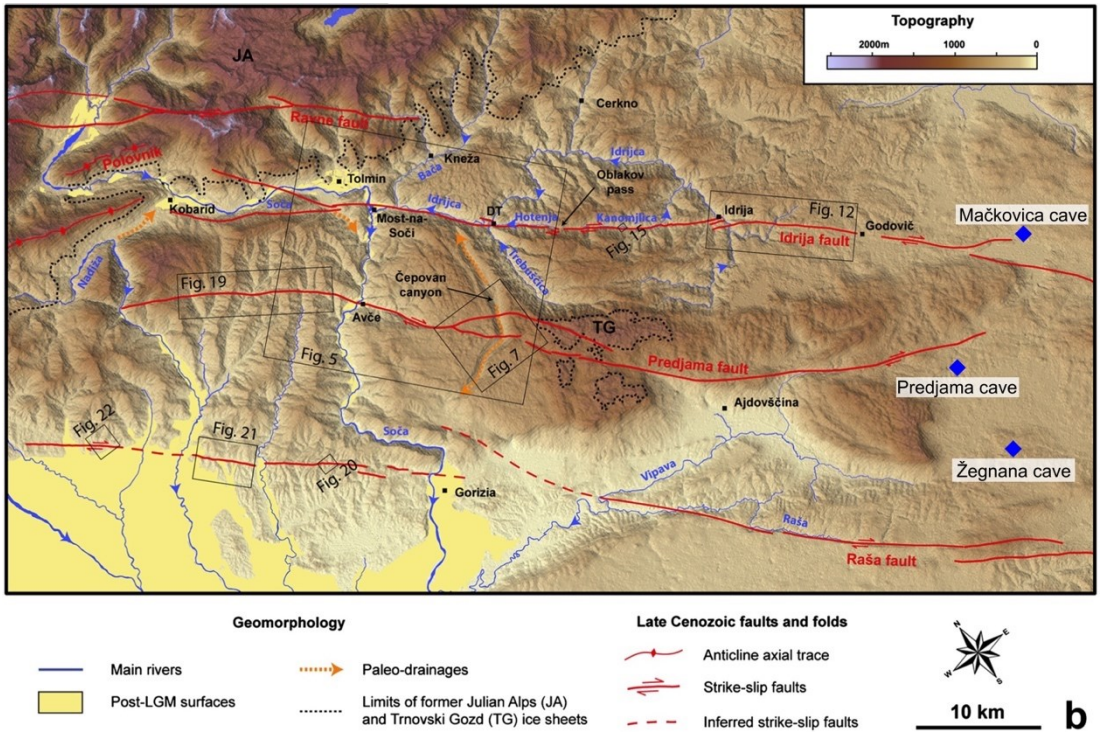

Fig. 9: Location of active faults within the Dinaric strike-slip system after Moulin(2016). The faults were defined as active due to their geomorphologic and geodetic properties.

There has been identification of numerous faults and geomorphologic markers from remote sensing such as satellite and high-resolution DEM datasets generated from airborne laser scanning. The identified faults show displacements ranging from a few meters to several kilometers. The Dinaric fault system is defined by NW-SE striking dextral strike-slip faults.

Ordered from NE towards SW the strike slip faults of the Dinaric fault system of western Slovenia (Fig. 9) are:

- Ravne fault (40 km) is subvertical dextral strike-slip fault.
- Idrija fault (124 km) is the longest fault of the system, it represents a subvertical dextral strike-slip fault with an average estimated slip rate of 1.0 mm/yr.

- Predjama fault (75 km) fault is a steeply NE-dipping dextral transpressive fault, with an average estimated slip rate of 0.7 mm/yr.
- Raša fault (87 km) is a subvertical dextral strike-slip fault with an average estimated slip rate of 0.7 mm/yr.

According to Atanackov et al. (2021) the aforementioned faults belong to the western set of the Dinaric fault system (Fig. 10).

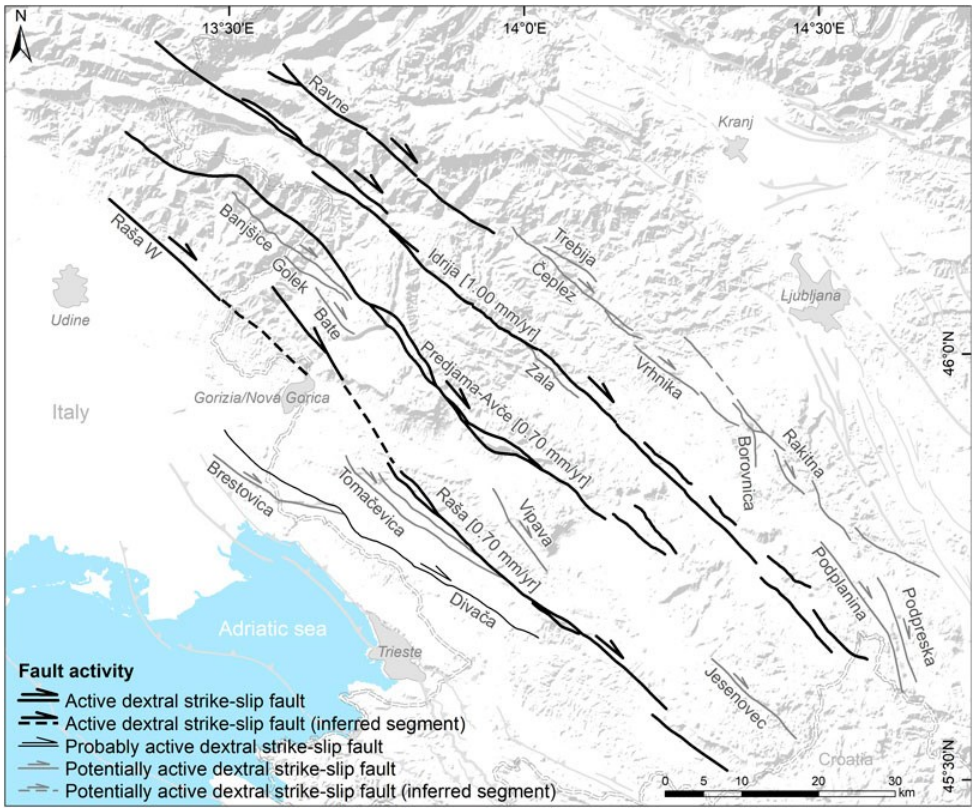

Fig. 10: Western Part of the Dinaric Fault System (Atanackov et al. 2021)

There is evidence of another existing seismogenic active fault, at the southern part of the studied Dinaric fault system, the so called Selce Fault in the Pivka basin. The fault was mapped as a ~15 km long structure. Near the village of Selce, a 4 km long, linear scarp is visible (Grützner et al. 2021b). The fault was recently found to be associated with a ~40 km long zone of microseismicity at depths of 5-18 km, which pointed to its

activity (Vičič et al., 2019). In 2008 and 2014, earthquakes with magnitudes of ML3.0 and ML4.7, showed a right-lateral focal mechanism (Vičič et al., 2019).

All of these faults show recent activity when judged from a geomorphological perspective. Along the Predjama fault there is a bend in the fault strike and a bifurcation into two branches. The general trend of the Predjama fault is parallel with the Idrija fault, which could mean that both could merge at depth (Moulin et al., 2016).

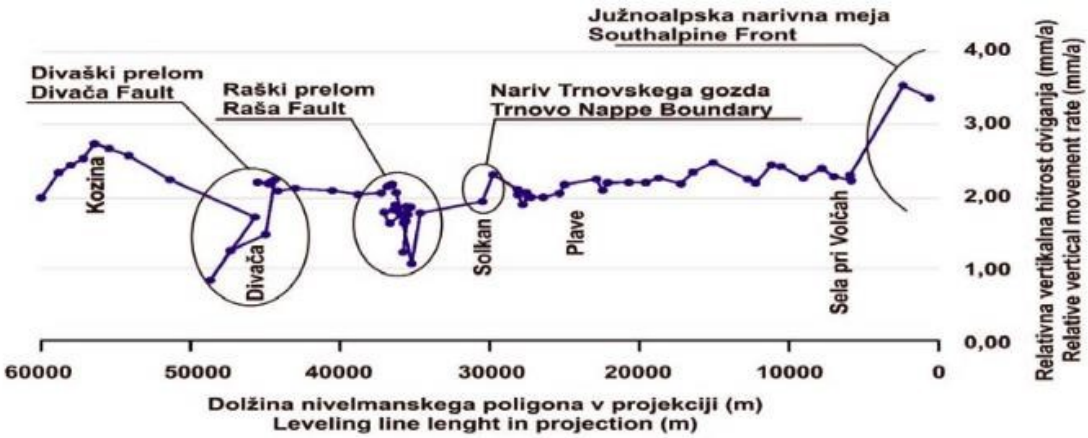

Fig. 11: Relative vertical movement rate over a part of the active faults of the Dinaric strike slip system derived from levelling line (Rižnar et al., 2007). There are clear changes are observed over Divača fault, Raša fault, Trnovo Nappe thrust fault and Southern Alps thrust front.

Geodetic measurements (Fig. 11) have been carried out in W Slovenia to cover tectonic structures (Rižnar et al., 2007). All of the major faults belonging to the Dinaric fault system have been observed using extensiometers for about 20 years and the measuring campaigns are still ongoing (Šebela, et al., 2021; Briestensky et al., 2015; Gosar et al., 2011; Gosar et al., 2009). All of these different measurements have showed that there is current micro-displacement activity along the major faults in the Dinaric fault system both in horizontal and vertical directions.

4.3 Known historic earthquakes in the area

While there are numerous known historic earthquakes from the study area (for a compilation see Vicic 2017), only a few of them have been observed as being recorded in the speleothems investigated in this study. For example, Šebela (2010) and references therein states, there is sufficient proof of broken speleothems as a co-seismic effect in Postojna cave during the 1st January 1926 earthquake (M=5.6). A newspaper reported a few days later after the earthquake that a massive stalagmite of almost 1 m in diameter collapsed due to the earthquake. The collapsed stalagmite was removed from the cave shortly after the event. A that time Zagreb seismic observatory determined the epicentral area of the earthquake to be in Cerknica polje. However, the Venice observatory calculated Postojna as the epicenter. The depth was estimated at around 17 km.

While this is not a common event in karst cave, it probably resulted because of the close proximity of the Postojna cave to the proposed epicenter. The epicenter was located either on the SE part of Idrija fault zone or in the Javorniki mountains.

For the other historic earthquakes, it is quite likely, that the source was too far from the investigated cave for the magnitude of the earthquake to have any significant effect on the speleothems.

In the following the two earthquakes which could be related to the dated disruption events in the investigated speleothems are described in more detail. These are the 1511 Idrija earthquake and the 1998 Bovec earthquake.

4.3.1 1511 Idrija Earthquake

The 1511 Idrija earthquake happened on 26th of March 1511 between 3 and 4 pm local time. According to Ribaric (1979), the event consisted of two earthquakes happening after each other. The center of the first event was NW of the town Tolmin which is situated on the border between Slovenia and Italy. The first event had M 6.9.

The second event had its center east of the city of Gemona in Friuli, Italy and is estimated to have had a magnitude of approx. 7.0 to 7.2.

All other sources except Ribaric (1979) only report one earthquake during this event. Later on this discrepancy was noted by Košir and Cecić (2011) who could show that the available historic information was not interpreted in a correct way by Ribaric. Fitzko et al. (2005) further discussed the problematics of two mainshocks vs. one main shock. They created a best fit scenario by doing modelling with synthetic earthquakes and comparing the results to reported intensities.

According to Fitzko et al. (2005) the most likely candidate was a right lateral strike slip earthquake along the Idrija fault with MW 6.9 with a 50-km long rupture, propagating towards NW. This is a likely result as similar hypotheses were found by other researchers such as Tiberi (2014). Bavec (2013) discussed a surface rupture which could also be observed in reality.

4.3.2 1956 and 1995 Ilirska Bistrica earthquakes

The 1956 Ilirska Bistrica earthquake occurred on the 31st January in 1956, and it was one of the most devastating earthquakes of the 20th century in Slovenia. With a magnitude of 5.1 and the intensity of VII EMS. The depth of the source was approximated at 7 km. The damage was mostly confined to the town and surroundings of Ilirska Bistrica, with 30% of buildings heavily affected, although the event was felt in a radius of about 140 km.

On 22nd of May 1995 two earthquakes occurred and they were ranked as some of the more devastating ones in the last 30 years. The first event had a magnitude of 4.4 and intensity of VI EMS, at the depth of 17 km. Just an hour later a second earthquake occurred with a magnitude of 4.7, with the intensity of VI EMS, at a depth of about 10 km. Around 80 aftershocks were reported in the following days.

The 1956 ML 5.1 Ilirska Bistrica earthquake might have been caused by the Raša fault (Ribarič, 1982). Two coseismic effects of 1995 Ilirska Bistrica in caves were reported (Šebela, 2010 and references in therein). In Dimnice cave a strong wind and a sound and splashing of water in the under-ground river were noticed by a group of cavers that were in the cave at that time. In the Zelše cave, a fallen rock hit a flowstone column about 1.3 m high and broke it off beneath the cave ceiling, causing the column to overturn.

4.3.3 1998 Bovec Earthquake

The “Bovec” earthquake occurred on the 12th of April 1998 at 10:55 am UTC and had a magnitude of M 5.7. The event happened along the Ravne fault in NW Slovenia. Intensities up to VIII EMS were reported in the area. The depth of the source was estimated at 8 km.

The earthquake caused damage to a number of buildings and triggered rockfalls. This geomorphologic change was supported by the relief in the mountainous area. After the main earthquake, a number of aftershocks with magnitudes up to M 4.2 occurred in a period of several weeks.

Bajc et al. (2001) relocated the 1998 sequence and gave a new depth of the center of around 7.6 km. They used the Joint Hypocentre Determination method for teleseismic events and suggested that there was a fault rupture with an upper boundary at 3 km along a length of 13 km. They reported that the rupture had a width of 7 km. According to Bajc et al. (2001) the rupture propagated in both directions which is also compatible with the aftershock distribution. Bressan et al. (2008) suggested that the fault zone is characterised by mechanical heterogeneities.

The surface of the area was studied by a group of geomorphologists (Cunningham et al. 2006). They used modern remote sensing data acquired using the LiDAR method. With the high resolution data available, they observed many splays along the Ravne fault with not so apparent strike-slip offsets. The Tolminka Springs basin close to the epicenters of both earthquakes was defined as a transtensional basin constructed in an overall transpressional system. No evident continuous surface trace of the Ravne fault

could be observed by Kastelic et al. (2008), instead at the surface they observed a fault zone of moderate to steep NE dipping fault planes at the surface, demonstrating thrust/reverse mechanisms.

After the 1998 earthquake another earthquake occurred in 2004. So far this was the last earthquake which was observed here.

The geological slip rate along the Predjama, Idrija and Raša fault is as an average over the last 255 ka estimated to range between 1.15 and 1.45 mm/yr, while the overall slip rate along the fault system is estimated to be 3.75 ± 0.6 mm/yr. There are changes in slip rates along different sites within the same segment, probably the slip towards the tips of the activated fault segment is lower (Moulin et al., 2016). Atanackov et al. (2021) approximated a slip rate of 2.5 mm/yr of dextral strike slip across the 25 km wide zone of the Predjama, Idrija and Raša fault.

5 Caves and Sampling

5.1 Sampled Caves and sample descriptions

In this study ten caves situated in Slovenia, north-western Dinarides, were visited and multiple samples were taken from these caves (Fig. 1). Primarily the selection of sampled cave was based on geographical location, their vicinity to the major seismically active NW-SE trending fault zones and their spatial distribution crosswise (SW-NE) the fault zones. Permitting the use of data for regional paleo seismic event interpretation in the study area. Secondarily it was based on the aforementioned factors which exclude deformed speleothems other than seismically deformed ones. All studied caves are formed within Jurassic carbonate rocks, mainly limestone (Fig. 3).

The sampling began in the spring of 2019 and ended in summer of 2021. All caves had one sampling campaign, except Divača cave which had two. The total number of sampled speleothems amounted to 90, 34 of which were dated until now. Samples from more recent cave sampling campaigns are expected to be tested. The caves, their basic information (according to the Slovenian cave cadastre, November 2021; cadastre number, coordinates, elevation of the entrance, length and depth) along with the sample quantities are to be found in the following tables (Table 1-Table 4):

Table 1: Visited Caves, geographic coordinates, elevation of the entrance and size of the caves.

Slovenian cave cadastre number	Name	D96 TM-E	D96 TM-N	Elevation of the entrance [m.a.s.l.]	Length [m]	Depth [m]
52	Mačkovica cave	443380	80158	479	807	45
311	Lipica cave	412973	61032	397	1400	250
734	Predjama cave	432119	75454	491	13877	168
736	Dimnice cave	425078	47526	565	6020	134
737	Vilenica cave	415228	59962	418	841	190
741	Divača cave	418258	60016	430	682	89
947	Vodnica cave	400392	70852	244	193	21
949	Pečina pod Medvejkom	409217	64061	344	70	18
960	Žegnana cave	433248	67851	590	492	62
13165	Bergevčeva cave	412293	62532	360	487	43

Table 2: Caves visited in 2019, number of samples taken

2019		
Cave	**Samples taken**	**Dated**
Divača cave	7	6
Divača cave	10	10
Vilenica cave	12	7
Lipica cave	7	2
Bergevčeva cave	8	7
Pečina pod Medvejkom	4	2
Total	**48**	**34**

Table 3:Caves visited in 2020, number of samples taken

2020	
Cave	**Samples taken**
Dimnice cave	11
Vodnica cave	5
Predjama cave	14
Mačkovica cave	10
Total	**40**

Table 4: Cave visited in 2021, number of samples taken

2021	
Cave	**Samples taken**
Žegnana cave	2
Total	**2**

5.1.1 Divača cave

Seven samples (*Fig. 12*) were taken from Divača cave (Divaška jama) during the first visit which took place on 2019-05-16. Of these seven samples six were dated at the University of Oxford. On a second visit on 2019-07-16, another ten samples were taken and all of them were dated. The sampled structures include secondary stalactites formed after the breakage of a stalactite, secondary stalactites formed on the bottom of an overturned stalagmite, small stalagmites growing on top of rock fall material, flowstone (speleothem) forming over clay rich slope deposits.

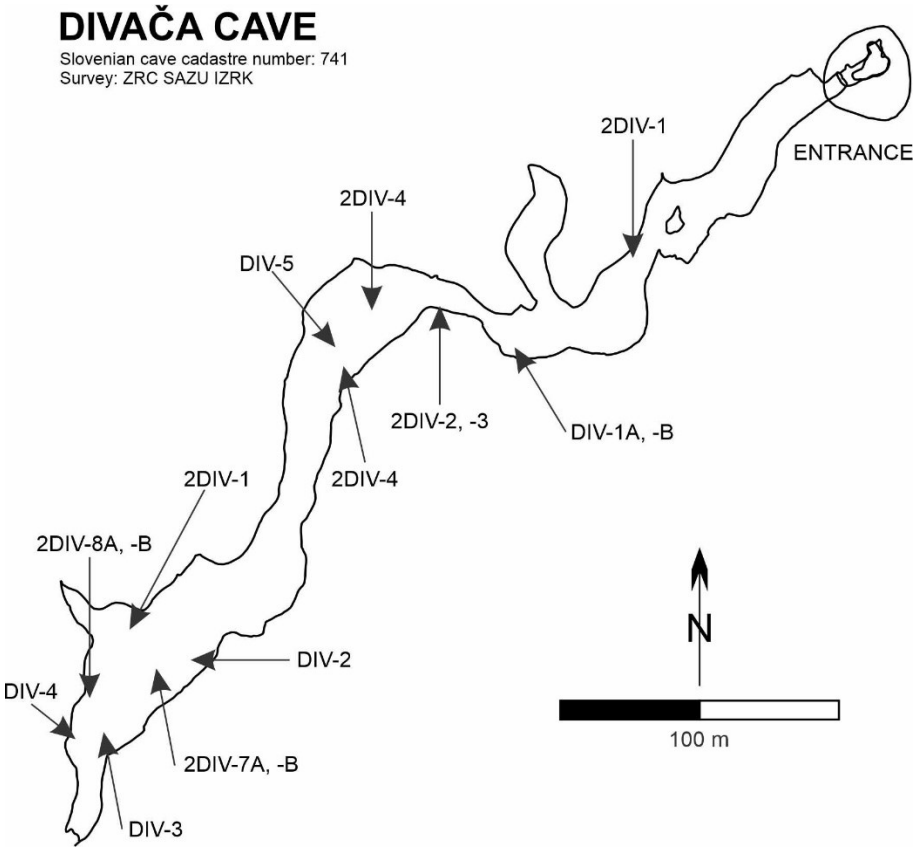

Fig. 12: Cave map of Divača cave, ground plan with marked sampling locations.

Table 5: Description of the samples from Divaska Cave

Sample number	Description of the sampling site
DIV-1A	Stalactite deposited post-collapse
DIV-1B	CaCO3 deposition over the break surface post-collapse
DIV-2	Large chamber collapse and sediment infill, covered with flowstone and stalagmites
DIV-3	Large collapsed blocks covered in speleothem
DIV-4	Broken block with previously growing stalagmite (tilted) and new stalagmite (straight)
DIV-5	Stalagmite from top of chamber collapse
2DIV-1	Secondary stalactite ("soda straw") growing after a fresh looking breakage of a stalactite
2DIV-2A	Secondary stalactite growing on the bottom part of an overturned stalagmite
2DIV-2B	Secondary stalactite growing on the bottom part of an overturned stalagmite
2DIV-3	Secondary stalactite growing after breakage of a stalactite
2DIV-4A	Small stalactites growing on the edge of collapsed host rock blocks
2DIV-4B	Small stalactites growing on the edge of collapsed host rock blocks
2DIV-4C	Small stalactites growing on the edge of collapsed host rock blocks
2DIV-4D	Small stalactites growing on the edge of collapsed host rock blocks
2DIV-4E	Small stalactites growing on the edge of collapsed host rock blocks
2DIV-4F	Small stalactites growing on the edge of collapsed host rock blocks
2DIV-5	Sase of 10 cm stalactites growing on the edge of collapsed host rock blocks
2DIV-6	Flowstone over the clay rich slope deposit that could be formed by a rockfall
2DIV-7A	Two breakages of stalagmites and two regrowth phases: older or 1st regrown stalagmite
2DIV-7B	Two breakages of stalagmites and two regrowth phases: younger or 2nd regrown stalagmite
2DIV-8A	Base of a 10 cm stalagmite on a collapsed stalagmite
2DIV-8B	Thin flowstone at the breakage on an vertically overturned stalagmite

Fig. 13: Large chamber collapse: sampled flowstone (1 DIV 2) at contact with the underlying collapse sediment

Fig. 14: "Soda straws" growing on a fresh looking breakage of a stalactite (2DIV-1).

Fig. 15: Small stalactite growing on the bottom part of an overturned big stalagmite (2DIV-2A).

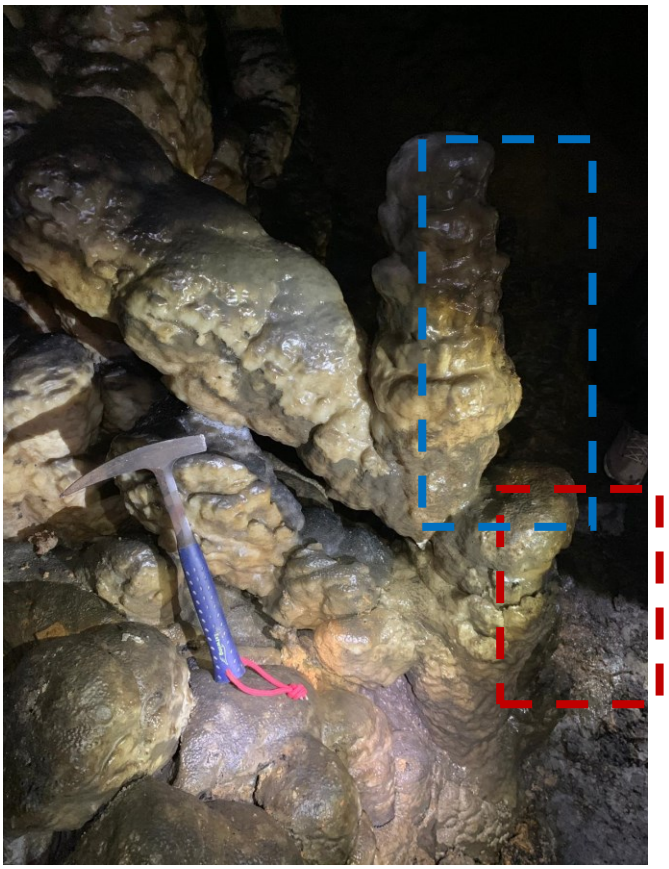

Fig. 16: Two generations of collapsed stalagmites. Red square is marking the older regrown stalagmite 2DIV-7A; blue square is marking the younger regrown 2DIV-7B.

5.1.2 Vilenica Cave

Vilenica Cave was visited on 2019-08-28 and 12 samples were taken from the cave (*Fig. 17*). Of these 12 samples, 7 were dated at the University of Oxford. In this cave stalagmites growing on broken stalagmites and stalagmites growing on rockfall material were sampled. In the cave, there are also columns, more than 2 m high, which are broken into several different pieces which are still standing on top of each other (for one example see *Fig. 18*). The breakage might be old while the speleothem infill of the cracks is still young. The structure might either be related to a single event or to multiple seismic events. There were also stalagmites growing on top of a number of broken stalagmites which seem to be broken in one single event.

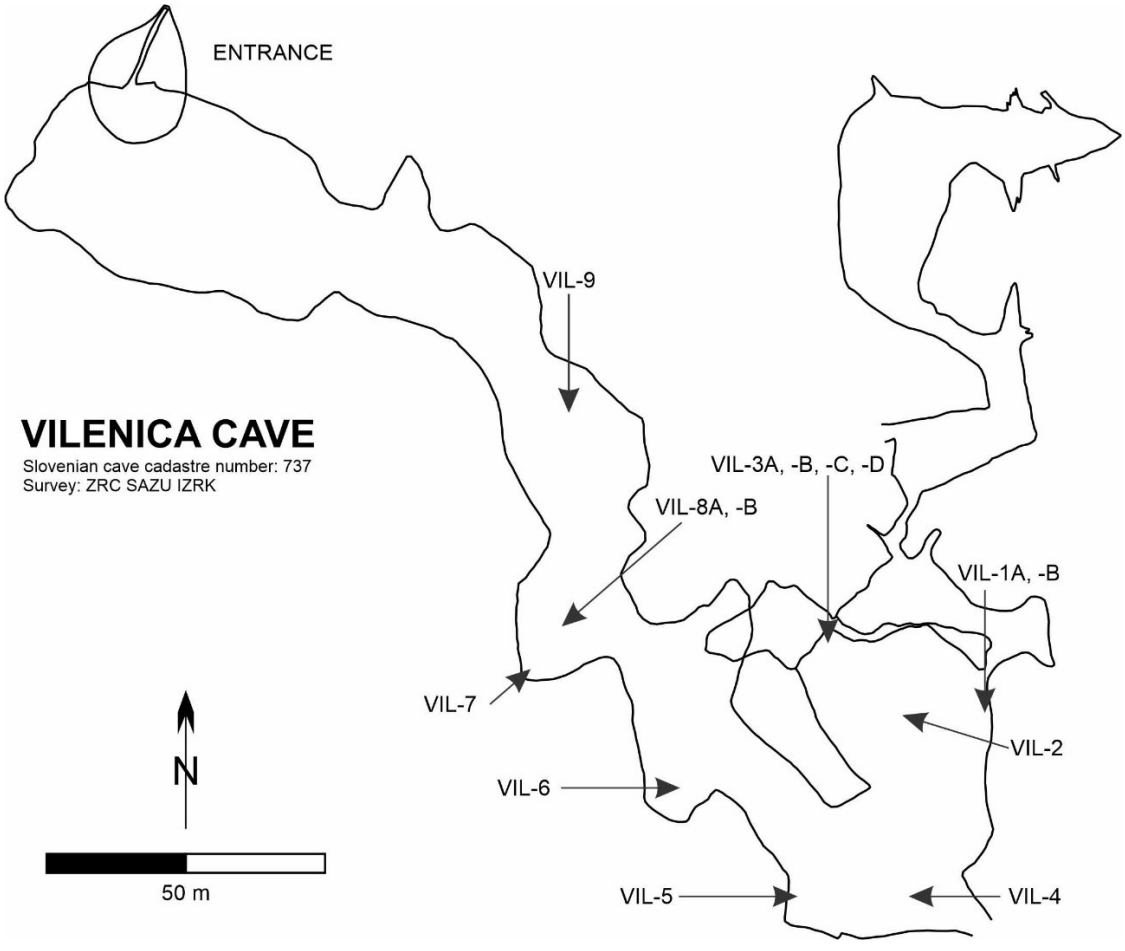

Fig. 17: Cave map of Vilenica cave, ground plan with marked sampling locations.

Table 6: Description of the samples from Vilenica cave.

Sample number	Description of the sampling site
VIL-1A	Base of a 30 cm stalagmite growing on a broken stalactite
VIL-1B	Base of a 35 cm stalagmite growing on a broken stalactite
VIL-2	Base of a 30 cm stalagmite growing on a broken stalagmite/stalactite
VIL-3A	Freshly healed crack in a column
VIL-3B	Freshly healed crack in a column
VIL-3C	Freshly healed crack in a column
VIL-3D	Freshly healed crack in a column
VIL-4	Base of a 50 cm stalagmite growing on a large broken stalagmite
VIL-5	Base of a small stalagmite growing on a broken stalagmite
VIL-6	Base of a 20 cm stalagmite growing on a broken stalactite
VIL-7	Tipped column that is fractured in the middle
VIL-8A	Freshly healed crack in a column
VIL-8B	Freshly healed crack in a column
VIL-9	Base of a 30 cm stalagmite growing on a broken stalagmite/stalactite

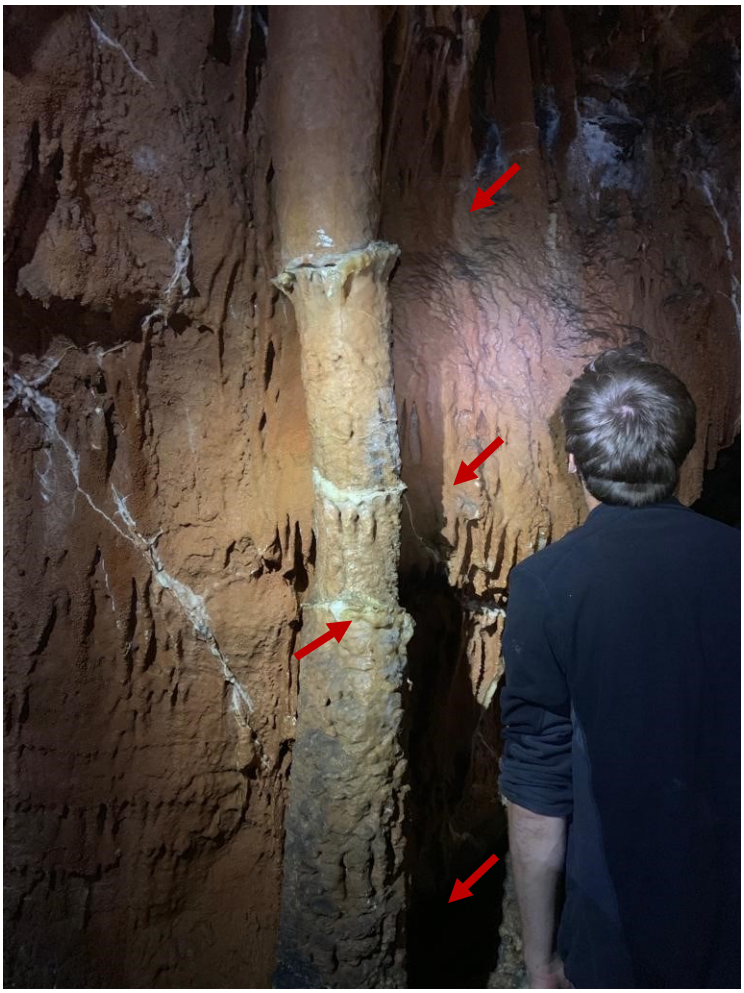

Fig. 18: Broken column in Vilenica Cave, red arrows are marking the infilled cracks.

5.1.3 Lipica

Lipica Cave was visited on 2019-09-22 (*Fig. 19*). On this occasion, seven samples were taken using a drill. Two of these seven samples were dated at Oxford university. The samples included stalagmites growing on top of previously broken stalagmites and stalagmites growing on top of rock fall.

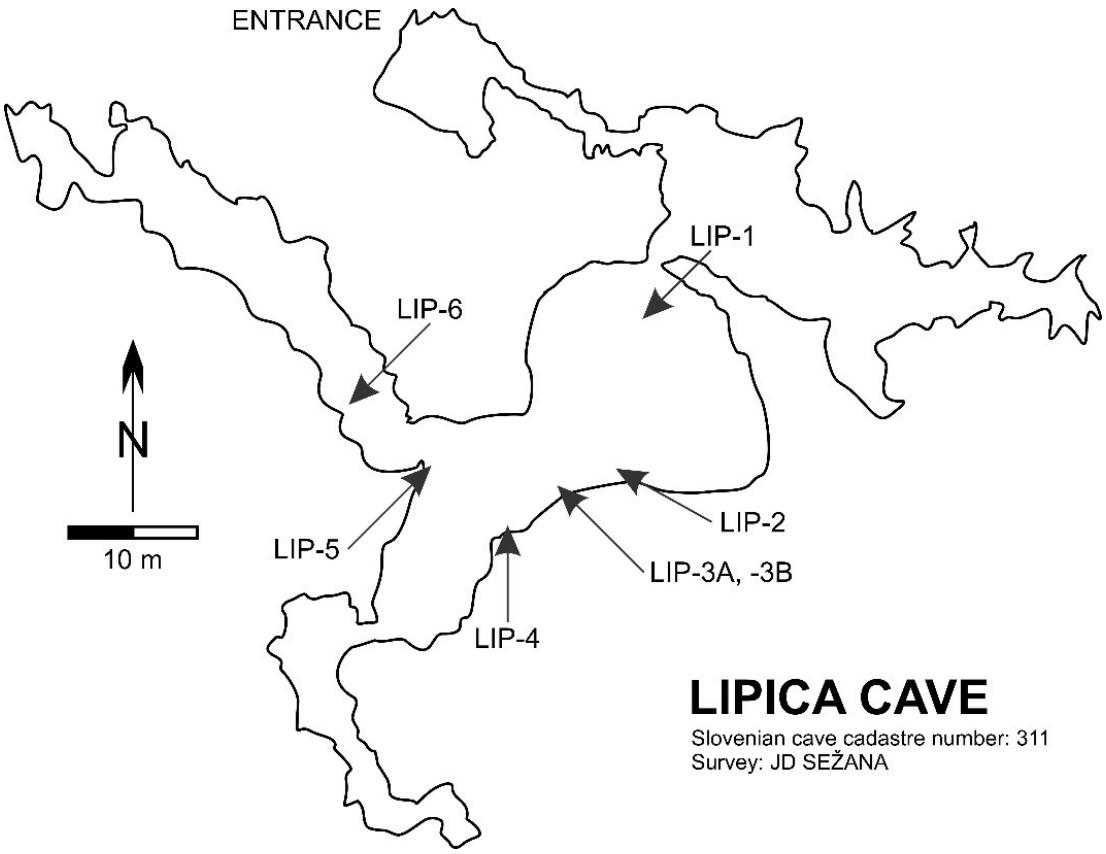

Fig. 19: Cave map of Lipica cave, ground plan with marked sampling locations.

Fig. 20: Sampled stalagmite (LIP-1) growing on a broken speleothem, either stalactite or stalagmite.

Fig. 21: Small stalactites (LIP-4) growing on the edge of a collapsed host block.

5.1.4 Bergevčeva cave

Bergevčeva Cave (*Fig. 22*) was visited on 2019-10-04. In the cave, 8 samples were taken using a drill and seven of the samples were dated at the University of Oxford.

In this cave, both stalagmites and stalactites were sampled. The stalagmites grow on top of broken and overturned stalagmites or on top of material which fell from the ceiling of the cave.

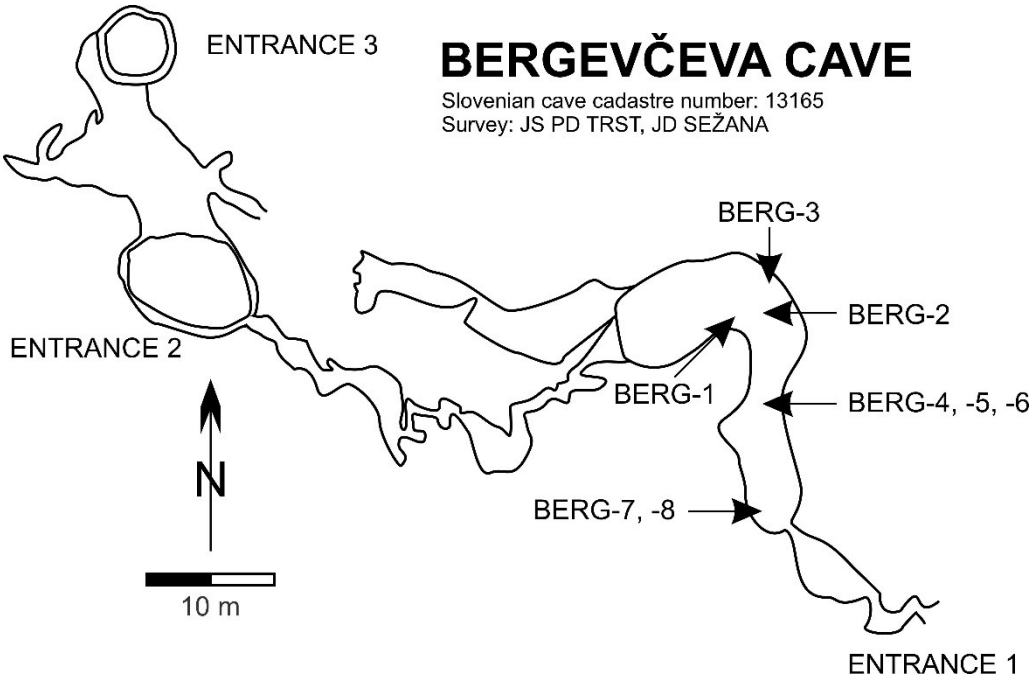

Fig. 22: Cave map of Bergevčeva cave, ground plan with marked sampling locations.

Table 7: Sample descriptions for the samples from Bergevceva cave

Sample number	Description of the sampling site
BERG-1	A long broken stalagmite at the edge of a small canyon
BERG-2	Numerous small stalactites growing from broken stalactite
BERG-3	15 cm stalagmite growing on top of a large stalagmite
BERG-4	Small stalagmite growing on top of material which fell from the ceiling of the cave
BERG-5	15 cm tall stalagmite growing on top of speleothem of unknown origin
BERG-6	Transponent 50cm tall stalagmite
BERG-7	Taken from a large column which is now a stalagmite as it was disconnected from the ceiling
BERG-8	Small stalagmite growing on top of sample Berg-7

Fig. 23: Sampled stalagmite (BERG-1), growing on a collapsed big stalagmite.

Fig. 24: Stalactites growing from a broken stalagmite in Bergevceva cave (BERG-2).

The stalactites grow from a broken stalagmite and have a size of about 2 cm (Fig. 24: Stalactites growing from a broken stalagmite in Bergevceva cave (BERG-2).There is also one sample (Berg-7) where limestone is deposited on top of a clay bed forming a column which was detached from the ceiling after the clay in the bottom has been eroded leading to a collapse of the bottom part of the column making it a stalagmite.

5.1.5 Pečina pod Medvejcom

The cave “Pecina Pod Medvejcem” was visited on 2019-10-04 (*Fig. 25*). Four samples were taken from the cave of which 2 were analyzed at the University of Oxford. The sampled speleothems are stalagmites which are growing on top of rock fall debris.

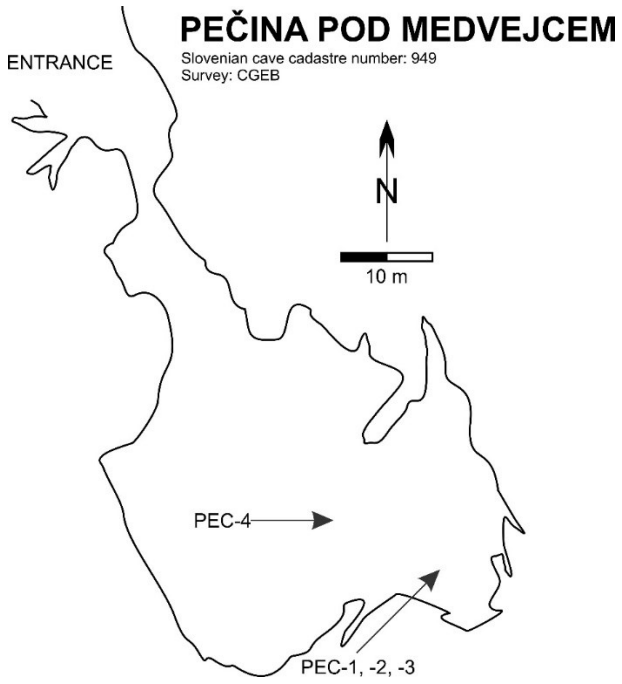

Fig. 25: Cave map of Pečina Pod Medvejcem, ground plan with marked sampling locations.

Fig. 26: Sampled small stalagmite (PEC-3), growing on a collapsed host rock boulder.

5.1.6 Dimnice

Dimnice cave was the first cave to be visited during 2020. The visit took place on 2020-01-30.

During the expedition to the cave, 11 samples were taken (*Fig. 27*).

The samples represent various different structures. While most of the samples consist of stalagmites growing on top of rock fall or broken speleothems, some other samples show more interesting pattern.

There is one chamber full of broken blocks on top of which numerous small stalagmites are growing. As the stalagmites grow on the same vertical axis (

Fig. 28) this could indicate that it is the same stalagmite growing which was interrupted by the falling block.

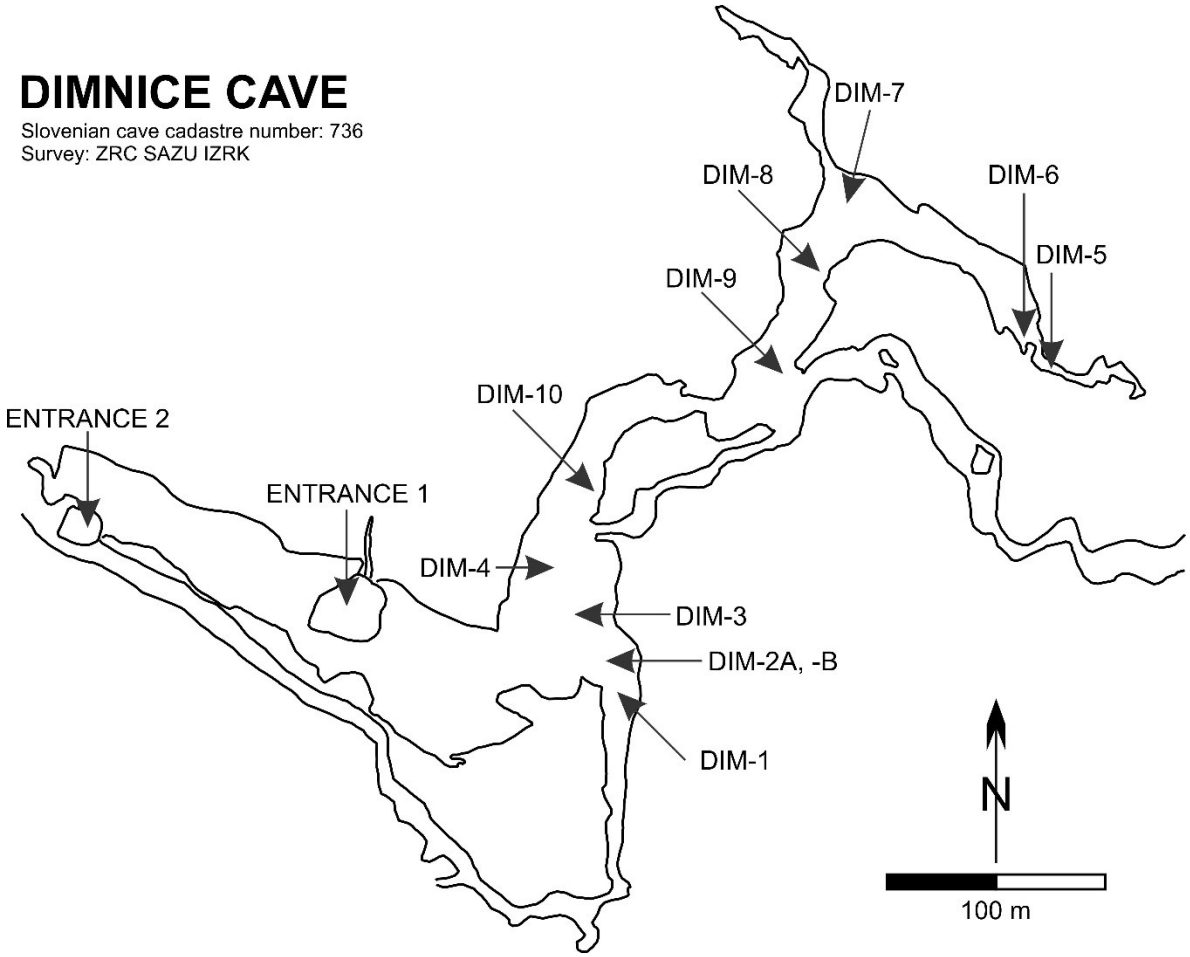

Fig. 27: Cave map of Dimnice cave, ground plan with marked sampling locations.

Table 8: Sample descriptions for the samples from Dimnice cave

Sample number	Description of the sampling site
DIM-1	Stalagmite growing on top of a boulder on a collapsed slope
DIM-2A	Taken from the foot wall of a collapsed rock
DIM-2B	
DIM-3	Small, still actively growing stalagmite on top of a collapsed boulder, 15 cm in diameter
DIM-4	Broken 2 m long stalagmite on which smaller ones are growing sample taken 20 cm from top of a small stalagmite
DIM-5	A large number of small stalagmites (up to 0.5 m tall) growing on top of a piece of broken flow stone
DIM-6	A stalagmite growing on top of a boulder
DIM-7	A room full of broken boulders on top of which numerous stalagmites are growing
DIM-8	Stalagmites growing on top of a collapse slope
DIM-9	Stalagmite growing on top of a large boulder
DIM-10	Stalagmite growing on boulder

Fig. 28: Stalagmites growing in same vertical axis (Dim-7).

5.1.7 Vodnica

During the cave visit on 2020-03-03, five samples were taken from Vodnica cave (*Fig. 29*).

Four of the samples represent stalagmites growing on top of collapsed blocks, while the fifth sample consists of a major collapse structure close to the smaller entrance to the cave.

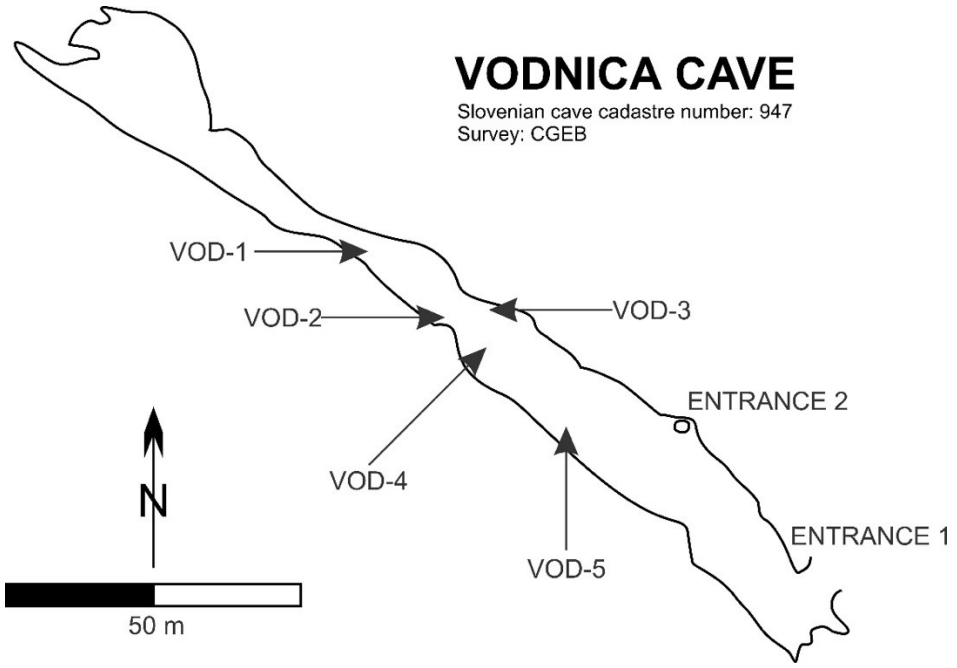

Fig. 29: Cave map of Vodnica Cave, ground plan with marked sampling locations.

Table 9: Sample descriptions for the samples from Vodnica cave

Sample number	Description of the sampling site
VOD-1	Still active stalagmite (approx. 20 cm tall) on top of collapsed boulder
VOD-2	Stalagmite growing on top of collapsed boulder in collapsed part of the cave
VOD-3	Small, still actively growing stalagmite, broken on top
VOD-4	Stalagmite growing on a 10-20 m diameter collapsed boulder
VOD-5	Taken on top of the major collapse structure close to the smaller entrance of the cave

5.1.8 Predjama

The visit to Predjama cave took place on 2020-07-30 and 14 samples were taken from the cave (*Fig. 30*). The majority of samples was taken in the big collapse chamber. Currently the samples are dated at the University of Oxford.

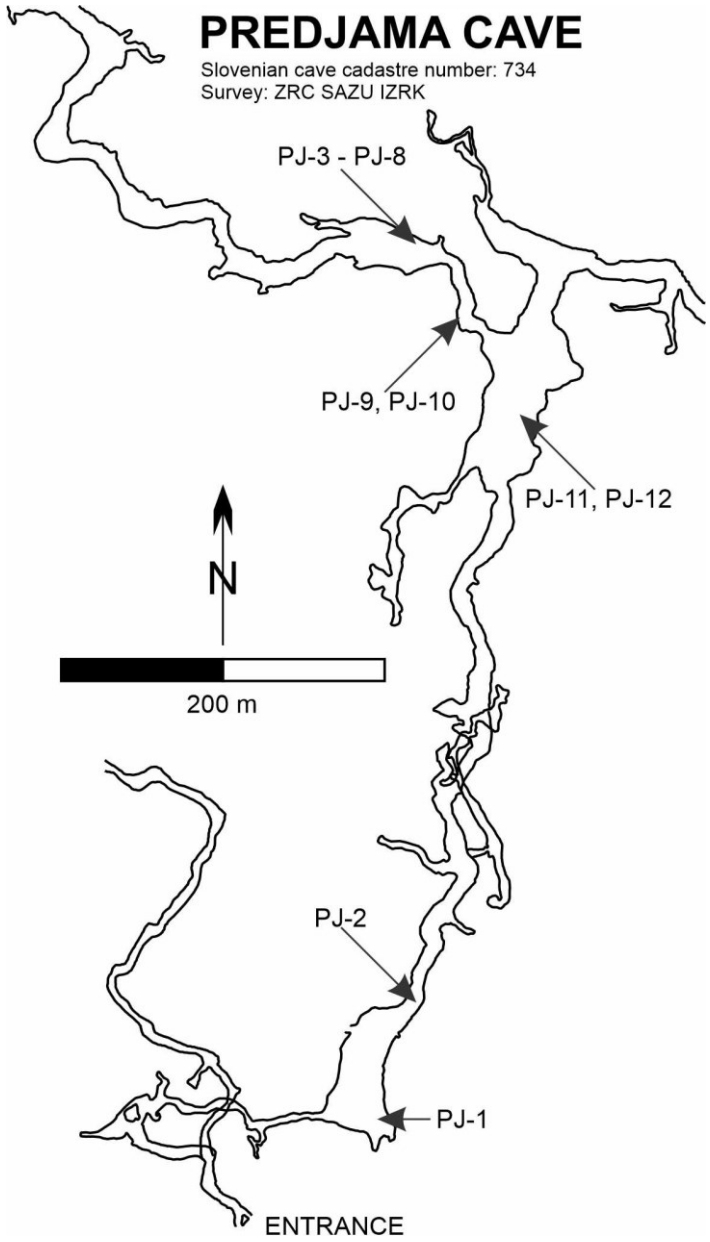

Fig. 30: Cave map of Predjama Cave, ground plan with marked sampling locations.

Table 10: Sample descriptions for the samples from Predjama cave

Sample number	Description of the sampling site
PJ-1	Sampled from a small stalagmite situated on a rock fall
PJ-2	Stalagmite growing on collapsed material A piece of stalagmite fell on it and is now being merged by a cover of flow stone
PJ-3	Situated in a chamber with rock fall. The chamber is full of stalagmites which are similar in size and up to 50 cm tall
PJ-4	
PJ-5	
PJ-6	
PJ-7	
PJ-8	

Fig. 31: Sampling in Predjama Cave.

5.1.9 Mačkovica cave

The Mačkovica cave was visited on 2020-08-10. During the expedition, 10 samples were taken using the cordless drill setup (*Fig. 31*). The majority of samples was taken in the big collapse chamber. While most of the samples represent stalagmites growing on rock fall or collapsed boulders, respectively, one sample (3M) represents a flow stone which is growing on a group of collapsed rocks.

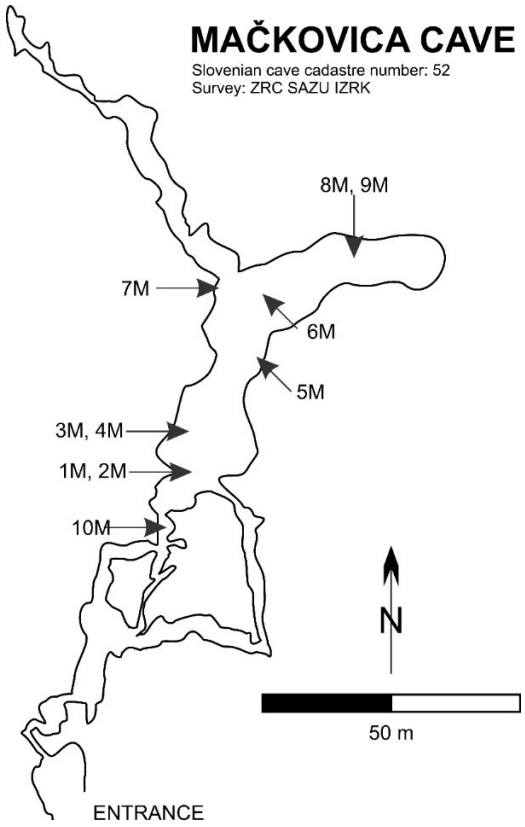

Fig. 32: Cave map of Mačkovica Cave, ground plan with marked sampling locations.

Table 11: Sample descriptions of Mackovica cave

Sample number	Description of the sampling site
1M	Base of a small stalagmite on a collapsed host rock boulder
2M	Base of a small stalagmite on a collapsed host rock boulder
3M	Base of a small stalagmite on a collapsed host rock boulder
4M	Base of a small stalagmite on a collapsed host rock boulder
5M	Base of a small stalagmite on a collapsed host rock boulder
6M	Base of a small stalagmite on a collapsed host rock boulder
7M	Base of a small stalagmite on a collapsed host rock boulder
8M	Base of a small stalagmite on a collapsed host rock boulder
9M	Base of a small stalagmite on a collapsed host rock boulder
10M	Base of a small stalagmite on a collapsed host rock boulder

Fig. 33: Sampled stalagmite in Mačkovica cave (5M).

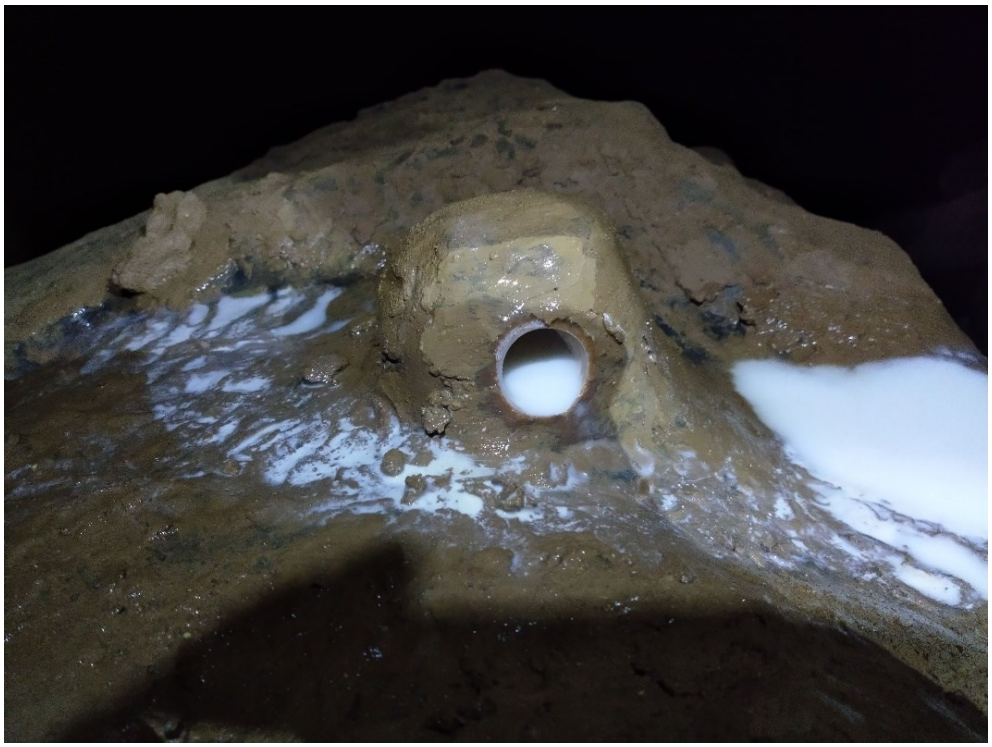

Fig. 34: Sampled stalagmite in Mačkovica Cave (7M).

5.1.10 Žegnana cave

During the expedition to Žegnana cave which took place on 2021-08-05, two samples from stalagmites growing on top of a rock fall, at the very end of the cave, were taken (*Fig. 35*).

Fig. 35: Cave map of Žegnana Cave.

Fig. 36: Sampled stalagmite in Žegnana Cave (ZEG-1).

5.2 Ages of sampled speleothems

The samples from the first visit to Divaska cave (2019-05-19) were dated by Franzi Lechleitner at Gideon Hendersons lab in Oxford.

These samples yielded the following results:

Table 12: Ages of the first Samples from Divaska Cave

Original name	U238 conc [ppm]	Th232 conc [ppb]	Corected age [years]			Initial (234U/238U)		
DIV-1-A-1	0,018	0,089	6629	±	442	1,012	±	0,008
DIV-1-B-1	0,502	1,826	7834	±	152	1,023	±	0,006
DIV-2-1	0,042	0,772	32510	±	806	0,954	±	0,007
DIV-2-2	0,073	1,873	29703	±	1009	0,935	±	0,006
DIV-3-1	0,005	0,253	out of range	±		out of range	±	
DIV-4-1	0,029	0,048	10085	±	269	1,035	±	0,006
DIV-5-1	0,047	0,077	3218	±	159	1,012	±	0,006

During a visit at the lab mentioned above in November 2019, 29 more samples have been dated by Donna M. Bou-Rabee.

The data are presented in Fig. 37.

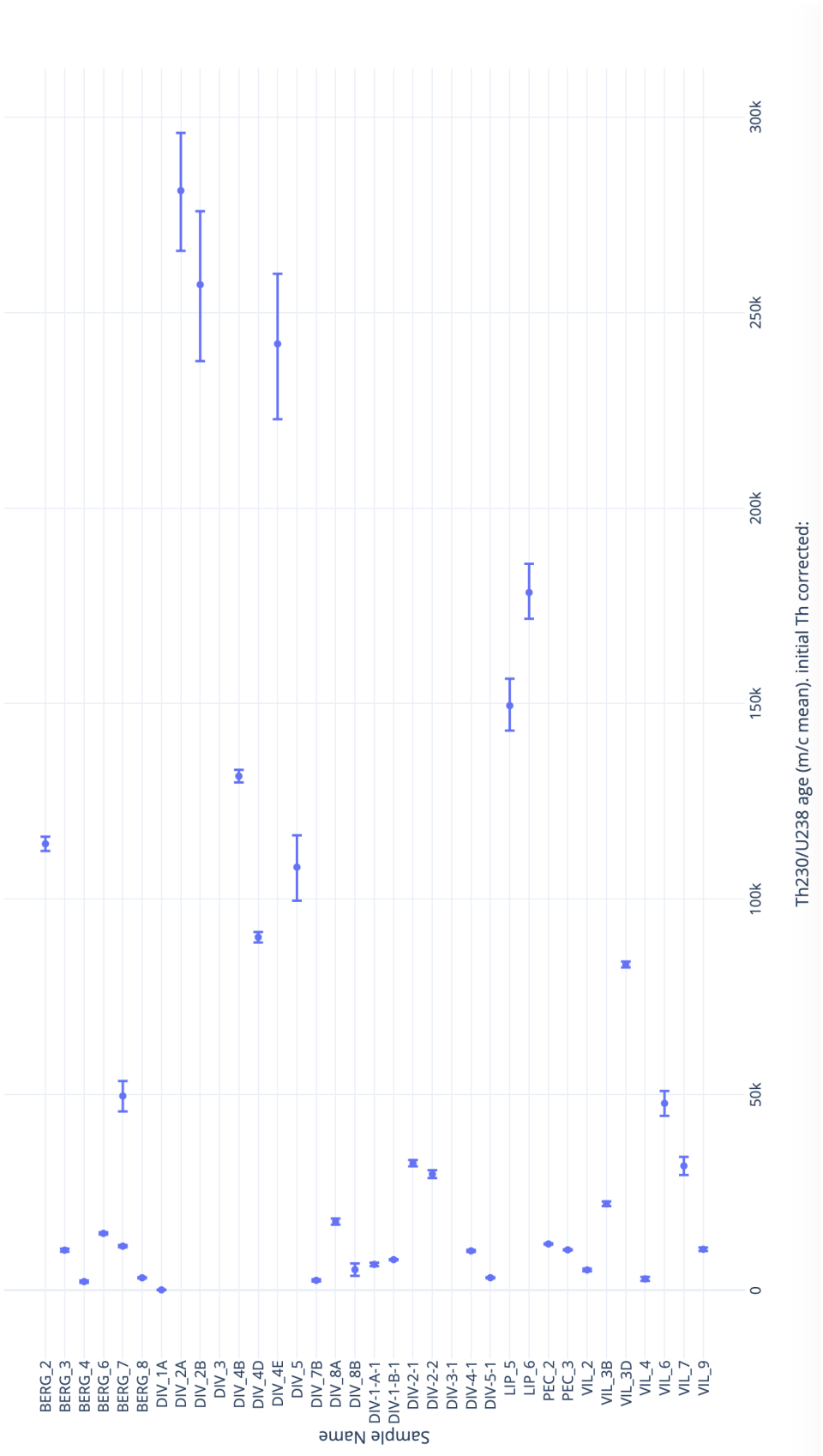

Fig. 37: Plot of all ages measured by F. Lechleitner and by Donna M. Bou-Rabee in November 2019.

There are several age clusters of which the most recent one (samples up to 20k year old) is the most interesting and is thus shown in more detail in Fig. 38.

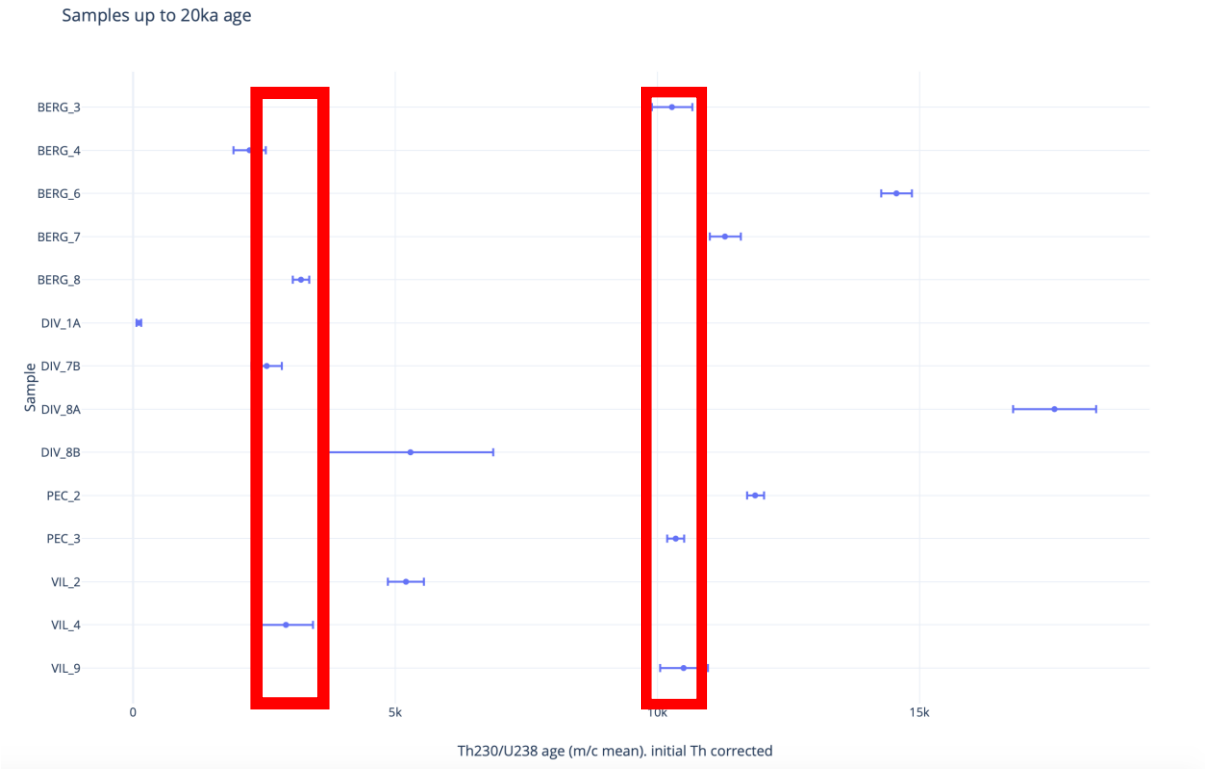

Fig. 38:Plot of ages up to 20kyr as measured by F. Lechleitner and by Donna M. Bou-Rabee in November 2019.

The geographic distribution of the two age clusters is presented in the following two maps:

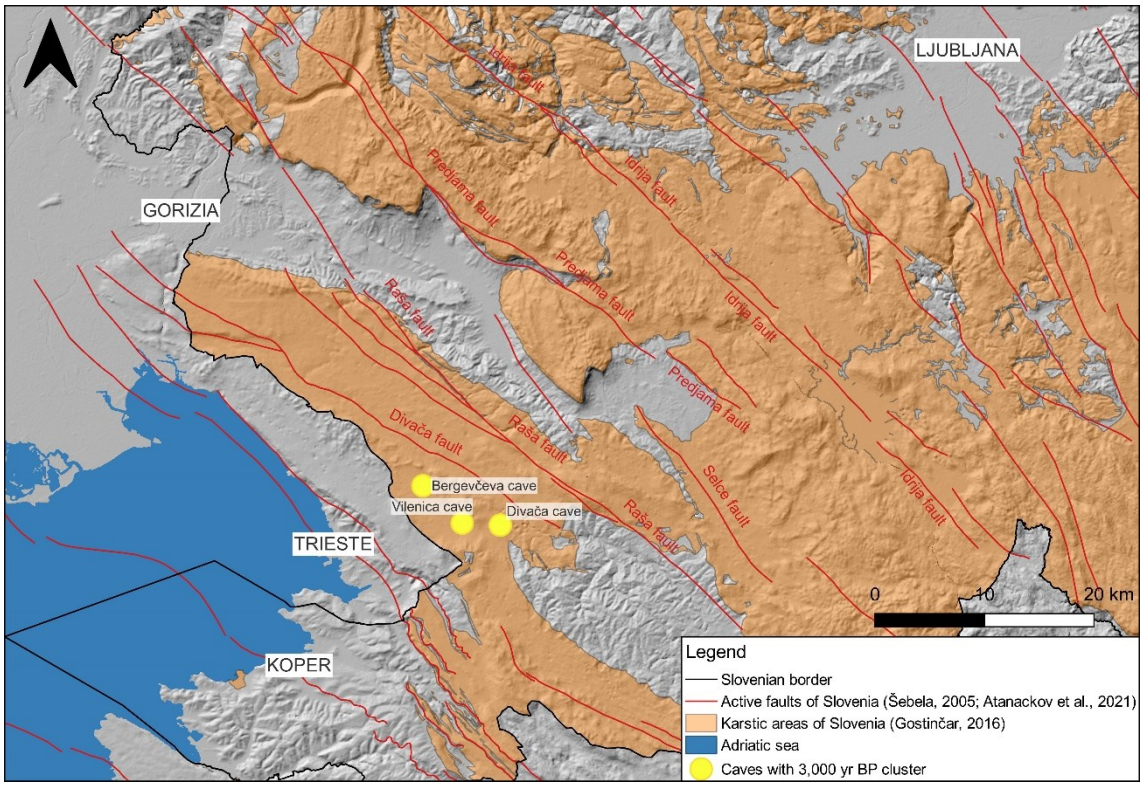

Fig. 39: Map displaying the caves where the samples within a 3,000 yr BP cluster were retrieved

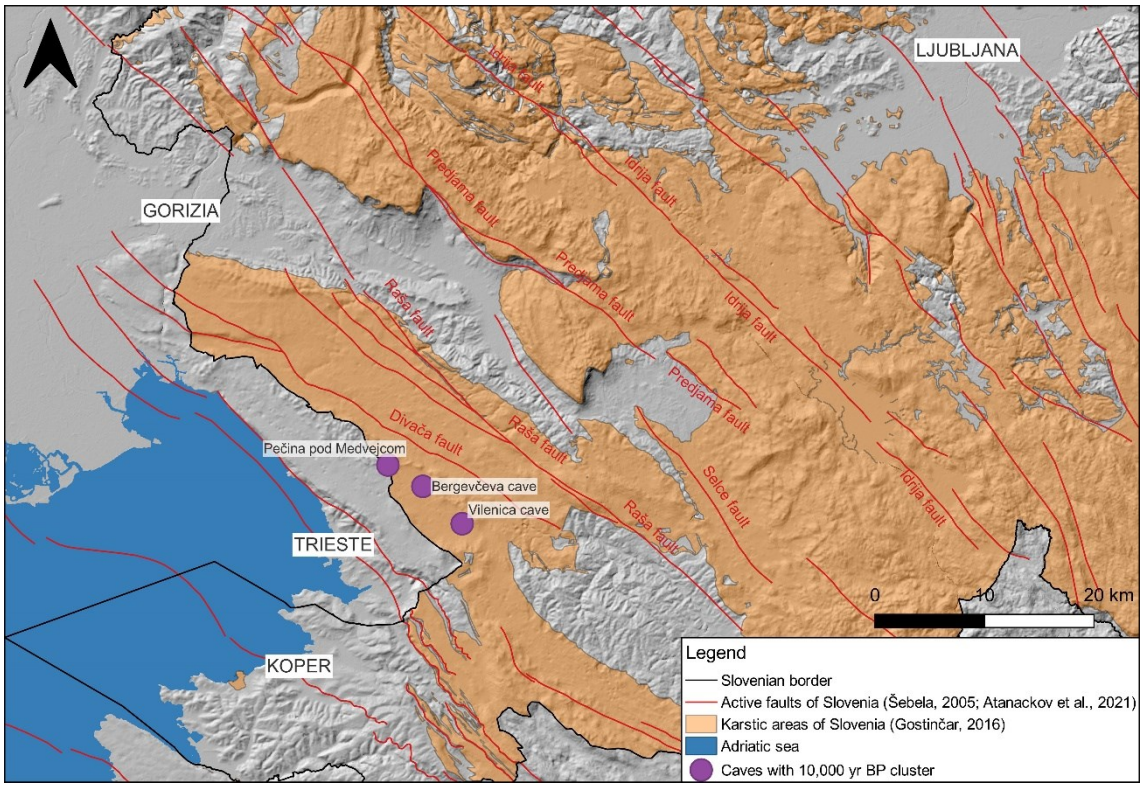

Fig. 40: Map displaying the caves where the samples within a 10,000 yr BP cluster were retrieved

6 Results, Discussion and Conclusions

Most of the dated samples show distinct ages with small error margins and can be used to distinguish between different events. In almost all of the caves there were two different age clusters, the older one of the identified clusters is around 10,000 yr BP, the younger one indicates an age of around 3,000 yr BP.

The age clusters of sampled speleothems could be indicative of large and destructive paleoearthquakes in the study area. Our results are correlated with newly reported paleoseismic events retrieved from paleoseismological trenching and highlight the importance of speleoseismology in complementing classical paleoseismology.

As can be seen from the graphs (Fig. 39 and Fig. 40), most of the samples analyzed in this study show distinct ages with relatively small error margins and can thus be used to distinguish between different events.

While there is a correlation between age and error margin in general, this correlation is not as strong when looking at the younger samples in more detail. This may indicate that there are also other significant influences on data quality and thus on the error margins than just the age of the samples. Such other factors may include inaccuracy in the field or in the laboratory, poorly chosen samples or other chemical properties of the minerals.

As an initial result we retrieve two distinct clusters of dates present in almost all of the caves. While the older one of the identified clusters is around 10,000 yr BP, the younger one indicates an age of around 3,000 yr BP.

The two distinct clusters could be indicative of large earthquakes in the study area. Our results are correlated with newly reported paleoseismic events retrieved from trenching and highlight the importance if speleoseismology in complementing classical paleoseismology.

Such clustering has also been reported from the Dead Sea Graben by Shmuel et al. (1996). They investigated laminated sediments from Lake Lisan (which represents the paleo-Dead Sea). In the sediments, they found distinct seismite bands, which they interpret as being formed on the sediment-water interface. They assume, that these have been formed during slip events. In their record, which they consider to be one of the longest on Earth, they found cluster in approx. 10kyr periods which are separated by quiet periods of similar length. They conclude that seismic hazard assessment should be based on records of at least 20 kyr length, otherwise one might miss the seismic event.

The distinct clusters also offer a possibility to indicate periods of higher seismic activity in the region and to distinguish between these more active periods and other periods which show a lower level of activity.

Specifically, speleoeseismology is important in an area like Northwestern Dinarides characterized by a large number of caves and where trenching is challenging because of the absence of fresh and recent sediments across active fault scarp.

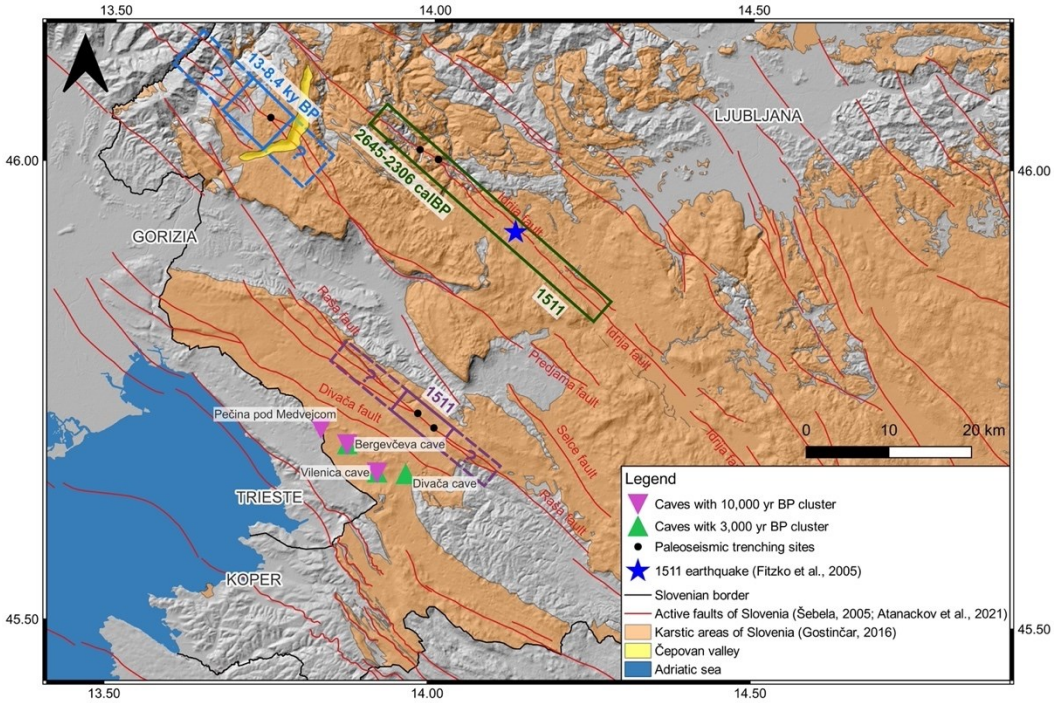

Fig. 41: Clusters of Earthquakes along Idrija, Divaca and Predjama faults

Table 13: Earthquakes in the area and their correlation to known faults with the assumption that our results refer to large magnitude earthquakes of the same order as the 1511main historical earthquake

Clustered along fault	Earthquake year and displacement	Magnitude	Source
Idrija	1511 ~2.5 m displacement	6.9	Fitzko et al. 2005, Aoudia et al., 2021
Rasa	1511 ~2.0 m displacement	6.5	Aoudia et al. 2021
Idrija	2kyr BP ~1 m displacement	6.0	Grützner et al. 2021
Idrija and Divaca	3kyr BP ~2.5 m displacement	large	This study
Predjama	8kyr BP ~1 m displacement	5.7	Grützner et al. 2021
Idrija and Divaca	10kyr BP ~2.5 m displacement	large	This study

In Table 13, further to the two newly identified paleoearthquakes inferred from this study we report a total of six large earthquakes that have been accommodated in the Dinaric Karst region with an estimated average displacement of 11.5 m over 10,000 years of time. This would correspond to an average co-seismic strain of ~1.2 mm/year during the last 10,000 years which is about 50% of the geodetic strain which equals to ~ 2 mm/year as inferred by recent GPS studies (Weber et al.2010; Metois et al.2015) and far less than geologic slip rates of ~ 3mm/year (e. g. Moulin et al., 2016 and Moulin and Benedetti, 2021). This would in turn mean that the active fault system in the Dinaric Karst is in a seismic slip deficit period therefore increasing the future hazard in the region.

Specifically, speleoeseismology is important in an area like North-western Dinarides characterized by vast karstic territories, a large number of caves and where trenching is challenging because of the absence of fresh and recent sediments across active fault scarp.

In summary, by using modern speleothem sampling, analysis and speleothem U/Th dating method, this study represents one of the first systematic speleoseismic studies in North-western Dinarides and in Slovenia, With around 6000 caves in the Dinaric Karst and Slovenia having more than 14,000 caves, the study represents a basis for future speleoseismic research in the study area. Research that has the possibility of increasing the understanding the characteristics of strong paleoearthquakes and modelling scenarios and in due course enhancing seismic hazard and risk assessment in North-western Dinarides.

7 Acknowledgements

I am out of words to express my gratitude for my supervisor, Prof. Abdelkrim Aoudia for his invaluable advice, patience, support and for encouraging me to always work harder as a single mother in a tremendously competitive scientific world.

Prof. Gideon Henderson and Dr. Franziska Lechleitner from the University of Oxford for the possibility to use their laboratory and for their support.

Prof. Stanka Sebela from the Karst institute for her help in the field and for sharing her extensive knowledge about my study area.

Both, Prof. Svante Björck from Lund University in Sweden and Prof. Sobhi Nasir from Sultan Qaboos University in Oman have given me valuable feedback and it has been much appreciated.

Post doc. assigned to my PhD project, Dr. Blaz Vicic and PhD candidate Uros Novak are thanked for helping me take samples in the caves and for being there during the field work.

All ICTP staff welcomed me to Trieste and made me feel like it was my second home. Finally for my friends, I couldn't have achieved this without them: Kilian Barth, Daniel Manu-Marfo, Marta D'Ambra, and most of all with all my heart Riccardo Delise.

My beautiful and smart siblings who are all over the globe but very close to me always, Noura, Nawaf, Khalid and Ahmed who I cherish with all my heart and have taught me to always strive for perfection and to work with diligence.

Finally, to my wonderful, beautiful, strong and smart mother, Professor Firyal Bou-Rabee who always pulled me up when I was down and pushed me to focus on my academics, who continues to remain my role-model. Most importantly to my son, Saud Al-Wazzan, his smile always made me work harder to achieve my goals and always soar higher.

8 References

Alfonsi and Cinti, 2021: Earthquake effects and insights on fault activity at the Beatrice Cenci cave (Abruzzo, Central Apennines). In: Annals of Geophysics, Vol. 64 no. 4, SE 435, p. 1-13.

Anderson & Jackson, 1987: Active tectonics of the Adriatic Region. Geophysical Journal of the Royal Astronomical Society, 91(3), 937–983. https://doi.org/10.1111/ j.1365- 246X.1987.tb01675. x

Akgöz & Eren, 2013: Traces of earthquakes in the caves: Sakarlak Ponor and Kepez Cave, Mersin, (southern Turkey). In: Journal of Cave and Karst studies, Vol. 77, no. 1, p. 63 - 74.

Aoudia et al., 2000: The 1976 Friuli (NE Italy) thrust faulting earthquake: a reappraisal 23 years later. Geophysical Research Letters, 27(4), 573–576.

Aoudia et al., 2021: Mechanics of the Raša fault and earthquake hazard on the city of Trieste. Conference talk at the 90° Congresso della Società Geologica Italiana, Trieste, 14th-16th of September, 2021.

Babek, et al. 2015: Pleistocene speleothem fracturing in the foreland of the Western Carpathians: a case study from the seismically active eastern margin of the Bohemian Massif, in: Geological Quarterly, 2015, Vol. 59 (3), p. 491–506 .

Bajc et al., 2001: The 1998 Bovec-Krn Mountain (Slovenia) Earthquake Sequence. Geophysical Research Letters, 28(9), 1839–1842.

Basili et al., 2013: The European Database of Seismogenic Faults (EDSF) compiled in the framework of the Project SHARE. URL: Http://diss. Rm. Ingv. It/share-Edsf.

Bechtold et al., 2009: Constraints on the active tectonics of the Friuli/NW Slovenia area from CGPS measurements and three- dimensional kinematic modeling. Journal of Geophysical Research, 114(B3), B03408. https://doi.org/10.1029/2008JB005638

Becker et al., 2005: Multiarchive paleoseismic record of late Pleistocene and Holocene strong earthquakes in Switzerland. in: Tectonophysics, Vol. 400, 1-4, p. 153 - 177.

Becker et al., 2006: Speleoseismology: A critical perspective. In: Journal of Seismology, Vol. 10, p. 371-388.

Becker et al., 2012: Active tectonics and earthquake destructions in caves of northern and central Switzerland. in: International Journal of Speleology, Vol. 41, no. 1, p. 35-49.

Benedetti et al., 2000: Growth folding and active thrusting in the Montello region, Veneto, northern Italy. Journal of Geophysical Research: Solid Earth, 105(B1), 739–766.

Bokelmann & Gribovszki, 2015: Constraints on Long-Term Seismic Hazard From Vulnerable Stalagmites. in: CSNI Workshop on "Testing PSHA Results and Benefit of Bayesian Techniques for Seismic Hazard Assessment" 4-6 February 2015, Eucentre Foundation, Pavia, Italy.

Bressan et al., 2007: Source parameters and stress release of seismic sequences occurred in the Friuli-Venezia Giulia region (Northeastern Italy) and in Western Slovenia. Physics of the Earth and Planetary Interiors, 160(3–5), 192–214. https://doi.org/10.1016/j.pepi.2006.10.005

Briestensky et al., 2015: Evidence of a plate-wide tectonic pressure pulse provided by extensometric monitoring in the Balkan Mountains (Bulgaria). Geologica Carpathica, 66(5), 427–438.

Burrato et al., 2008: Sources of M w 5+ earthquakes in northeastern Italy and western Slovenia: An updated view based on geological and seismological evidence. Tectonophysics, 453(1), 157–176.

Buser, 2009: Geological Map of Slovenia, 1:250.000.

Di Domenica & Pizzi, 2017: Defining a mid-Holocene earthquake through speleoseismological and independent data: implications for the outer Central Apennines (Italy) seismotectonic framework. in: Solid Earth, Vol. 8, p. 161 - 176.

Caporali et al., 2013: Modeling surface GPS velocities in the Southern and Eastern Alps by finite dislocations at crustal depths. Tectonophysics, 590, 136–150. https://doi.org/10.1016/j.tecto.2013.01.016

Delaby, 2001: Palaeoseismic investigations in Belgian caves. in: Netherlands Journal of Geosciences / Geologie en Mijnbouw, Vol. 80, no. 3-4, p. 323 - 332.

Fitzko et al., 2005: Constraints on the location and mechanism of the 1511 Western-Slovenia earthquake from active tectonics and modeling of macroseismic data. Tectonophysics, 404(1), 77–90.

Forti, 2001: Seismotectonic and Paleoseismic Studies from Speleothems: The State of the Art. in: Geologica Belgica, vol. Karst and Tectonics, 4/3-4: 175 - 185.

Forti & Onac, 2016: Caves and Mineral Deposits. in: Zeitschrift für Geomorphologie, Vol. 60, Suppl. 2, p. 57-102.

Galadini et al., 2005: Seismogenic sources potentially responsible for earthquakes with M≥ 6 in the eastern Southern Alps (Thiene-Udine sector, NE Italy). Geophysical Journal International, 161(3), 739–762.

Gilli, E. 1999: Evidence of palaeoseismicity in a flowstone of the Observatoire cave (Monaco), in: Geodinamica Acta Vol. 12, issue 3-4, p. 159-168.

Gosar et al., 2011: On the state of the TM 71 extensometer monitoring in Slovenia: seven years of micro-tectonic displacement measurements. Acta Geodyn Geomater, 8(4), 389–402.

Gosar et al., 2009: Surface Versus Underground Measurements of Active Tectonic Displacements with TM 71 Exstensometers in Slovenia. Acta Carsologica, 38(2–3).

Gospodaric, R., 1964: Sledovi tektonskih premikov iz ledene dobe v Postojnski jami.- Naše jame 5 (1963), 5-11, Ljubljana.

Gospodarič¬, R., 1968: Podrti kapniki v Postojnski jami.- Naše jame 9 (1-2), 15-31, Ljubljana.

Grenerczy et al., 2000: Present crustal movement and strain distribution in Central Europe inferred from GPS measurements. Journal of Geophysical Research: Solid Earth, 105(B9), 21835–21846.

Gribovszki et al., 2018: Numerical Modeling of Stalagmite Vibrations. In: Pure and Applied Geophysics, 175, 4501-4514.

Grützner, C., et al., 2021: Holocene surface-rupturing earthquakes on the Dinaric Fault System, western Slovenia: Solid Earth, Vol. 12, pages 2211–2234.

Kagan et al., 2005: Dating large infrequent earthquakes by damaged cave deposits. in: Geology, Vol. 33 no. 4, p. 261 - 264.

Kagan, 2012: Multi-site late Quaternary paleoseismology in the Dead Sea transform region: Independent recording by lake and cave sediments. Ministry of Energy and Water Resources-Geological Survey of Israel.

Kagan et al., 2017: Broken speleothems reveal Holocene and Late Pleistocene paleoearthquakes in Northern Calabria, Italy. in: Quaternary International, Vol. 451, p. 176 - 184.

Kastelic et al., 2004: Seismotectonic characteristics of the 2004 earthquake in Krn mountains. Potresi v Letu, 78–87.

Kastelic et al., 2008: Neo-Alpine structural evolution and present-day tectonic activity of the eastern Southern Alps: the case of the Ravne Fault, NW Slovenia. Journal of Structural Geology, 30(8), 963–975.

Kempe, 2004: Natural Speleothem Damage in Postojnska Jama, Slovenia, Caused by Glacial Cave Ice? A First Assessment. in: Acta Carsologica, Vol. 33 No. 1, p. 266 - 290.

Kempe et al., 2009: Glacial cave ice as the cause of widespread destruction of interglacial and interstadial speleothem generation in Central Europe. in: White, W. B. (ed.): Proceedings of the 15th International Congress of Speleology, Kerrville, TX, vol.. 2, p. 1026-1031.

Kranjc, A., (ed), 1997: Slovene Dinaric Karst, Kras. ZRC SAZU.

Lacave et al., 2000: Measurement of natural frequencies and damping of speleothems. in: Proceedings of the 12th World Conference on Earthquake Engineering, Auckland, New Zealand, Sunday 30 January - Friday 4 February 2000, abstract no. 2118.

Lacave et al., 2004: What can be concluded about seismic history from broken and unbroken speleothems? in: Journal of Earthquake Engineering vol. 8, no. 3, p. 431-455.

Lang et al., 2021: Macro-characterisation of cave damage for palaeoseismological investigations in regions of low strain: A case study from centralewestern North Island (Waitomo caves), New Zealand. in: Quaternary Science Reviews Vol. 272, 107202, p. 1-28.

Lippitsch, R., 2003: Upper mantle structure beneath the Alpine orogen from high-resolution teleseismic tomography. Journal of Geophysical Research, 108(B8), 2376. https://doi.org/10.1029/2002JB002016

McCalpin (ed.), 2009: Paleoseismology. Academic Press /Elsevier, Burlington.

Mendecki & Szczygiel, 2019: Physical Constraints on speleothem deformations caused by earthquakes, seen from a new perspective: Implications for paleoseismology. In: Journal of Structural Geology, Vol. 126, 146-155.

Metois, M. et al., 2015. Insights on continental collisional processes from GPS data: dynamics of the peri-Adriatic belts, J. geophys. Res.: Solid Earth, 120(12), 8701–8719.

Moulin, A., 2014: Active tectonics of the Alps-Dinarides junction: quantitative morphology, fault kinematics and implications for the Adria microplate geodynamics. Doctoral Thesis.

Moulin et al., 2016: The Dinaric fault system: Large-scale structure, rates of slip, and Plio-Pleistocene evolution of the transpressive northeastern boundary of the Adria microplate. Tectonics, 35(10), 2258–2292.

Moulin & Benedetti, 2021: Fragmentation of the Adriatic Promontory: New Chronological Constraints From Neogene Shortening Rates Across the Southern Alps (NE Italy). In: Tectonics, Vol. 37, Issue 9, 3328 – 3348.

Nocquet, J. M., 2012: Present-day kinematics of the Mediterranean: A comprehensive overview of GPS results. Tectonophysics, 579, 220–242.

O'Brien, P.J., 2001: Subduction followed by collision: Alpine and Himalayan examples. Physics of the Earth and Planetary Interiors, 127(1–4), 277–291. https://doi.org/10.1016/S0031- 9201(01)00232- 1

Panno et. al, 2009: Major Earthquakes Recorded by Speleothems in Midwestern U.S. Caves. in: Bulletin of the Seismological Society of America, Vol. 99, No. 4, pp. 2147–2154.

Placer, 1999: Contribution to the macrotectonic subdivision of the border region between Southern Alps and External Dinarides. Geologija, 41(1998), 223–255.

Placer, 2008: Principles of the tectonic subdivision of Slovenia. Geologija, 51(2), 205–217.

Placer et al., 2010: The bases for understanding of the NW Dinarides and Istria Peninsula tectonics. Geologija, 53(1), 55–86.

Poljak et al., 2000: The seismotectonic characteristics of Slovenia. In Seismic Hazard of the Circum-Pannonian Region (pp. 37–55). Springer.

Postpischl et al., 1991: Palaeoseismicity from karst sediments: the “Grotta del Cervo” cave case study (Central Italy). in: Tectonophysics, Vol. 193, no. 1, p. 33 - 44.

Rajendran et al., 2016: Stalagmite growth perturbations from the Kumaun Himalaya as potential earthquake recorders. in: Journal of Seismology Vol. 20, p. 579-594.

Ribaric, 1982: Seismicity of Slovenia; catalogue of earthquakes (792 AD--1981). Seizmološki zavod SR Slovenije.

Riznar et al. 2007: Recentna aktivnost regionalnih geoloških struktur v zahodni Sloveniji. Geologija, 50(1), 111–120.

Sasowski et al., 2003, Concurrent tectonism and aquifer evolution >100,000 years recorded in cave sediments, Dinaric karst, Slovenia. in: Environmental Geology, Vol. 44, p. 8-13.

Sebela, 2008: Broken speleothems as indicators of tectonic movements. in: Acta Carsologica, Vol. 37 no. 1, p. 51-62.

Sebela, 2010: Effects of earthquakes in Postojna cave system. in: Acta Carsologica, Vol. 39 no. 3, p. 597-604.

Sebela et al., 2021: *Micro-displacement monitoring in caves at the Southern Alps–Dinarides–Southwestern Pannonian Basin junction*. In: Bulletin of Engineering Geology and the Environment, Vol. 80, 7591 – 7611.

Shanov, S., Kostov, K., 2015: Dynamic Tectonica and Karst. Springer-Verlag Berlin Heidelberg.

Shmuel et al., 1996: Long-term earthquake clustering: A 50,000-year paleoseismic record in the Dead Sea Graben. In: Journal of Geophysical Research: Solid Earth, Vol 101, B3, 6179-6191.

Spötl & Mattey, 2012: Scientific drilling of speleothems – a technical note. in: International Journal of Speleology, Vol. 41, p. 29 - 34.

Stampfli et al., 1998: Subduction and obduction processes in the Swiss Alps. Tectonophysics, 296(1–2), 159–204. https://doi.org/10.1016/S0040-1951(98)00142-5

Stampfli & Borel, 2002: A plate tectonic model for the Paleozoic and Mesozoic constrained by dynamic plate boundaries and restored synthetic oceanic isochrons. Earth and Planetary Science Letters, 196(1–2), 17–33.https://doi.or g/10.1016/S0012-821X(01)00588- X

Szczygiel et al. 2021: Quaternary faulting in the Western Carpathians: Insights into paleoseismology from cave deformations and damaged speleothems (Demänová Cave System, Low Tatra Mts. in: Tectonophysics, Vol. 820, p. 229111.

Vicic, B., 2017: High resolution earthquake relocation along Idrija fault system in Western Slovenia and its application in understanding the deformation along the active faults of NW External Dinarides, PhD-Thesis.

Vicic et al., 2019: Geometry and mechanics of the active fault system in western Slovenia. In: Geophysical Journal International, Vol. 217 Issue 3, 1755-1766.

Vrabec & Fodor, 2006: Late Cenozoic tectonics of Slovenia: structural styles at the Northeastern corner of the Adriatic microplate. The Adria Microplate: GPS Geodesy, Tectonics and Hazards, 151–168.

Weber et al., 2010: GPS-derived motion of the Adriatic microplate from Istria Peninsula and Po Plain sites, and geodynamic implications. Tectonophysics, 483(3), 214–222.

Woodhead et al., 2016: Developing a radiometrically-dated chronologic sequence for Neogene biotic change in Australia, from the Riversleigh World Heritage Area of Queensland. in: Gondwana Research Vol. 29, p. 153-167.

Xueqin & Fudong: Damaged Speleothems of the Ms 8.0 Wenchuan Earthquake, China, and the Implications for Seismology. in: Geophysical Research Abstracts, Vol. 19, EGU General Assembly 2017.

Zivcic et al., 2014: Temporary seismological measurements in the Postojna Cave System. in: Acta Carsologica, Vol. 43 no. 1, p. 149-157.

Zupancic et al., 2001: The earthquake of 12 April 1998 in the Krn Mountains (Upper Soča valley, Slovenia) and its seismotectonic characteristics. Geologija, 44(1), 169–192.

Web pages without Author

http://www.speleothemscience.org/who/, accessed 2018-08-11

https://www.earth.ox.ac.uk/research-groups/isotopes-and-climate/people/, accessed 2018-08-15